2008-11-14

Wire-Braced Semirigid Elevated Rotor System Concept for a Human-Powered Helicopter

Jonathan Richard Silvester
Brigham Young University - Provo

WIRE-BRACED SEMI-RIGID ELEVATED ROTOR SYSTEM

CONCEPT FOR A HUMAN-POWERED HELICOPTER

by

Jonathan R. Silvester

A thesis submitted to the faculty of

Brigham Young University

In partial fulfillment of the requirements for the degree of

Master of Science

School of Technology

Brigham Young University

December 2008

BRIGHAM YOUNG UNIVERSITY

GRADUATE COMMITTEE APPROVAL

of a thesis submitted by

Jonathan R. Silvester

This thesis has been read by each member of the following graduate committee and by majority vote has been found to be satisfactory.

Date	Mike P. Miles, Chair

Date	A. Brent Strong

Date	W. Jerry Bowman

BRIGHAM YOUNG UNIVERSITY

As chair of the candidate's graduate committee, I have read thesis of Jonathan R. Silvester in its final form and have found that (1) its format, citations, and bibliographical style are consistent and acceptable and fulfill university and department style requirements; (2) its illustrative materials including figures, tables, and charts are in place; and (3) the final manuscript is satisfactory to the graduate committee and is ready for submission to the university library.

_____   _____
Date   Mike P. Miles
                                        Chair, Graduate Committee

Accepted for the School

                                        _____
                                        Barry M. Lunt
                                        Graduate Coordinator

Accepted for the College

                                        _____
                                        Alan R. Parkinson
                                        Dean, Ira A. Fulton College of Engineering
                                        and Technology

ABSTRACT

WIRE-BRACED SEMI-RIGID ELEVATED ROTOR SYSTEM

CONCEPT FOR A HUMAN-POWERED HELICOPTER

Jonathan R. Silvester

School of Technology

Master of Science

In order for a human-powered helicopter (HPH) to fly, lifting the weight of its human pilot-engine and the weight of its own structure, the rotary wings need to be extremely large and exceptionally lightweight. Through centuries of dreaming and decades of modern attempts, no design so far has been able to obtain the combination of an adequately large rotor size, sufficiently lightweight structure, and an inherently stable aircraft. This thesis describes a concept of a wire-braced semi-rigid elevated rotor system for a proposed HPH. Then, using scale models and quantitative analysis, tests a series of supporting hypotheses in order to prove that such a large rotor system could be sufficiently lightweight, maintain its geometry to overcome coning and twisting, avoid interplanar interference, produce sufficient lift, yield inherent aircraft stabilty, and demonstrate that the drag penalty induced by external bracing wires would be more than offset by the benefits of wire bracing.

ACKNOWLEDGMENTS

I am foremost thankful to the creator of the universe and its several flying creatures. Not a day goes by that I do not see either a soaring bird or hovering insect and wonder how they do it so well.

I am also thankful for family members who have fostered creativity and education throughout my life. I thank my parents who provided me with books, educational opportunities, creative toys, and a safe place to grow up. And I am deeply thankful for the love and encouragement of my wife, Kimberli; she truly supports me in all I do and has been a key inspiration for me to both start and ultimately finish this thesis. Thank you for waking up at 3:00 a.m. to help tie delicate wire-bracing knots on my rotor models.

Lastly, I want to thank the good faculty members of my thesis committee. I thank Dr. Mike Miles, my committee chair, who helped shape my abstract ideas into an actionable thesis project. I thank Dr. Brent Strong, who teaches and inspires scientific creativity in every lecture and every conversation. And I thank Dr. Jerry Bowman, who helped work through the aerodynamic principles, including the strengths and potential weaknesses of my ideas, and who always encourages the work of research and testing both in the lab and in the air.

TABLE OF CONTENTS

LIST OF TABLES

LIST OF FIGURES

1 Introduction

No human-powered aircraft has ever been able to takeoff vertically from a stationary position, to climb to a height of even just a few meters and hover stably for more than a few seconds, and to do so wholly unaided by any external person or energy storage device.

Many have tried. The earliest and most famous design for a human-powered helicopter (HPH) was sketched in the late fifteenth century by Renaissance artist/inventor Leonardo da Vinci as shown in Figure 1-1.
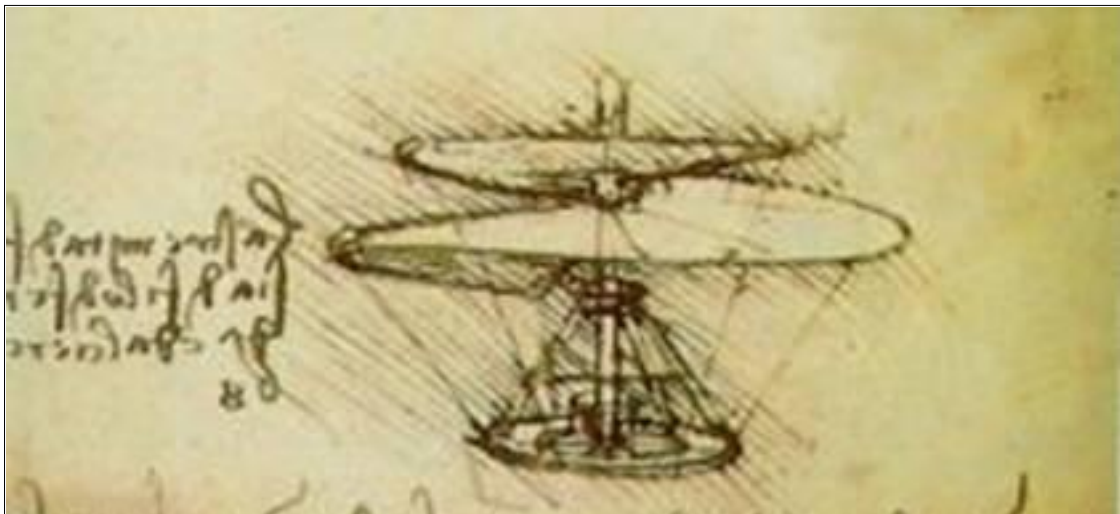
Figure 1-1 Leonardo da Vinci's sketch "Aerial Screw" (American 2008)

Though conceptually ingenious and centuries ahead of his time, da Vinci's design, like so many others since, fails to translate sufficient amounts of the human power into work done on the atmosphere to create lift.

Unlike birds, who are physiologically built for flight with nearly hollow bones and disproportionately large chest muscles, humans are hearty earthbound folk, with solid bones and with a more distributed muscle system. Human-powered flight requires the aid of external apparatus, chiefly by way of artificial wings.

In the past three decades, much progress has been made in the realm of human-powered flight. Innovative teams have created wonderful airplanes with wingspans as wide as jetliners and with an empty aircraft weights only half that of their human pilots. Many of these have flown quite successfully. The MIT Daedalus shown in Figure1-2 holds the current world record both distance and duration with its 119km flight over the Mediterranean from the island of Crete to the shore of Santorini. (www.dfrc.nasa.gov)

Figure 1-2 MIT Daedalus Human-powered Airplane (Dryden 2008)

Despite the many successes of the human-powered airplanes, human-powered helicopters have not progressed as far, facing several additional problems and design requirements beyond those of their fixed-wing counterparts. While airplanes are allowed as much runway as necessary to build up speed to takeoff, a comparable vertical lift aircraft needs to liftoff from a stationary point.

What's more, a human-powered vertical lift aircraft is required to hover stably over a fixed point. This is a far less efficient method of flight than flying horizontally, which is why hummingbirds are so remarkable in the class of birds

Of the dozens of modern attempts that have been made to takeoff vertically, most never get off the ground; all prove to be too heavy, too unstable, and/or too inefficient in their rotor systems.

1.1 Statement of the Problem

The chief constraint of an HPH is the tremendously unfavorable power-to-weight ratio of its human engine-pilot. At best, even a world-class athlete still needs a vehicle with a rotor diameter several times larger than a conventional helicopter yet one that weighs less than his/her own bodyweight. With limited power from such a relatively heavy source, the necessary rotor diameter of a potentially feasible aircraft would need to be so large and the total structure would need to be so very lightweight that any such machine, while theoretically possible, is "practically impossible for conventional designs." (Filippone 2002).

While the power generated by human beings varies from person to person, the ideal maximum potential power from perfectly fit world-class athletes has been studied

extensively. Maximum power output decreases over time, ranging from over 1000W (about 1.3 horsepower) for 10-12 seconds, such as sprinting up a flight of stairs, to approximately 300W (about 0.4 horsepower) sustained up to 8 hours (see Figure 1-3). And while body mass also varies from person to person, an average weight for this class of athlete is around 650N (approximately 65kg of force or 143 lbs.). (Filippone 2002)
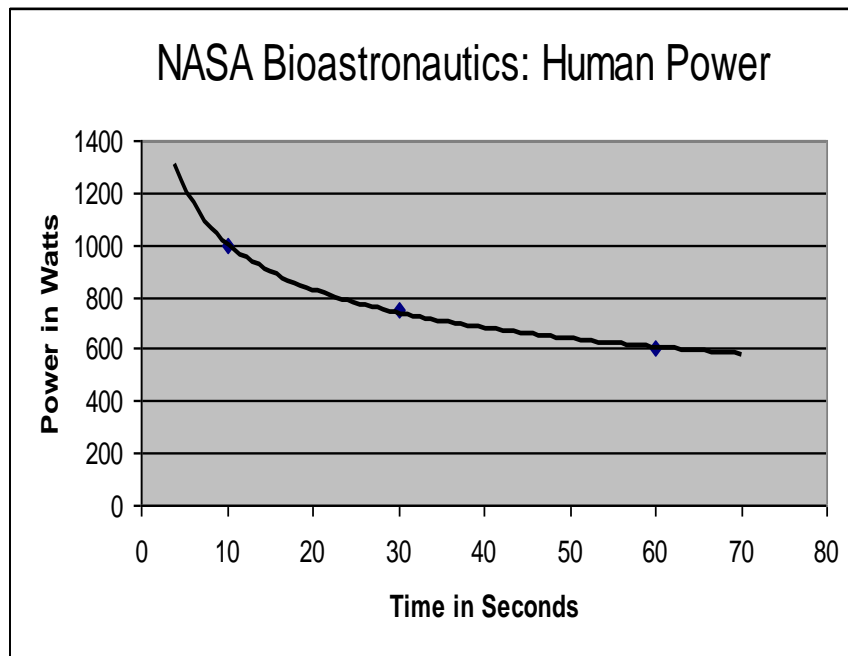
Figure 1-3 Human Power over Time

1.1.1 Lost Lift—Wing Coning

To some degree, wing coning is a phenomenon on all helicopter rotors but is greatly exaggerated on lightweight HPH rotors. It is the result of lift forces distributed along the rotors that creates a bending moment about the hub. Such coning compromises lift by reducing the rotor disk area and by unproductively directing a component of wing-

lift inward rather than entirely upward as shown in Figure 1-4. Additionally, the bending stresses the rotor structure.

Da Vinci II attempt in 1987.
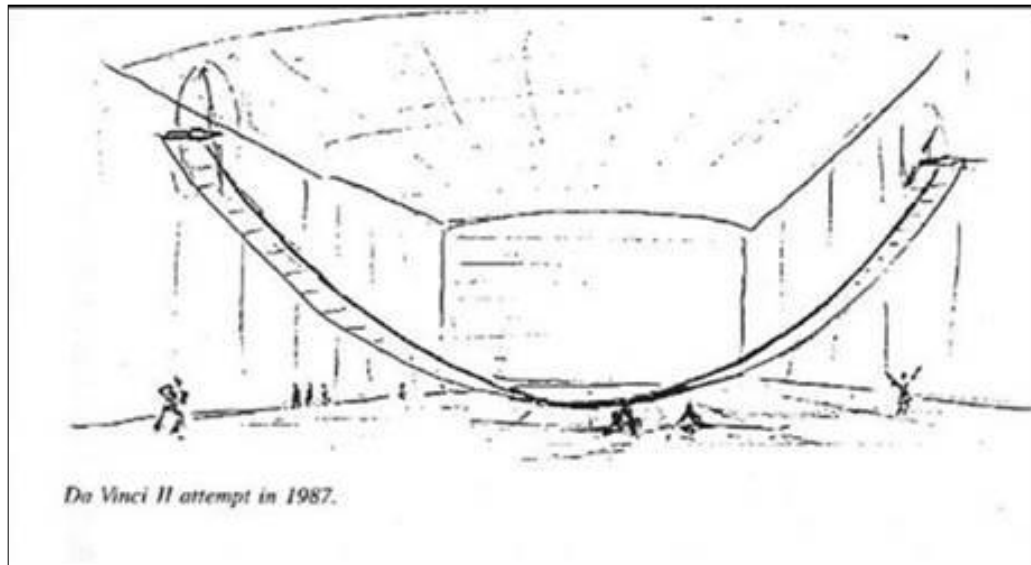
Figure 1-4 Example of Typical Wing Coning of an HPH: Cal Poly Da Vinci II (Drees 1993)

- *Inefficient Rotors:* Conventional rigid helicopter rotor blades require blade twist along the span of the airfoil to smooth the distribution of lift in order to reduce the coning of the rotor system as shown in Figure1-5. The blade twist gives the slower inner portion of the blade greater pitch for increased lift, and the faster outer portion of the blade provides flatter pitch for less lift. This design technique is suboptimum because it does not utilize the maximum lift/drag angle attack at every point along the rotor span, especially the outer regions of the rotor. (Fundamentals 1998)
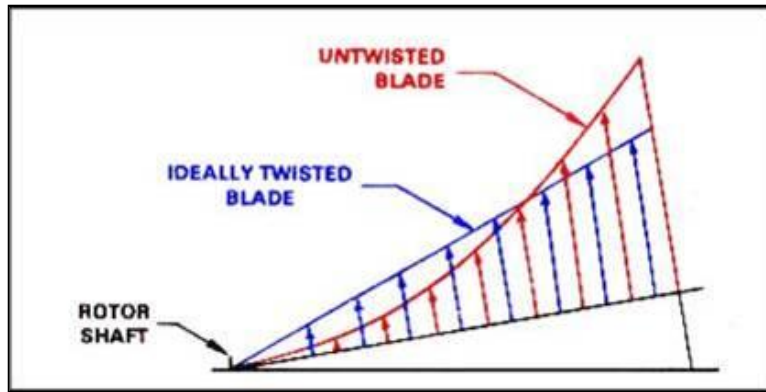
Figure 1-5 Distribution of Lift on Twisted and Untwisted Blades (Fundamentals 1988)

- *Inherent Instability*. In their efforts to maximize the benefits of flight in ground effect (a more efficient cushion of air created between the ground and the airfoil), most modern HPH designs have had very low rotor systems whose center of gravity (CG) is close to and sometimes above the center of lift as shown in Figure 1-6.
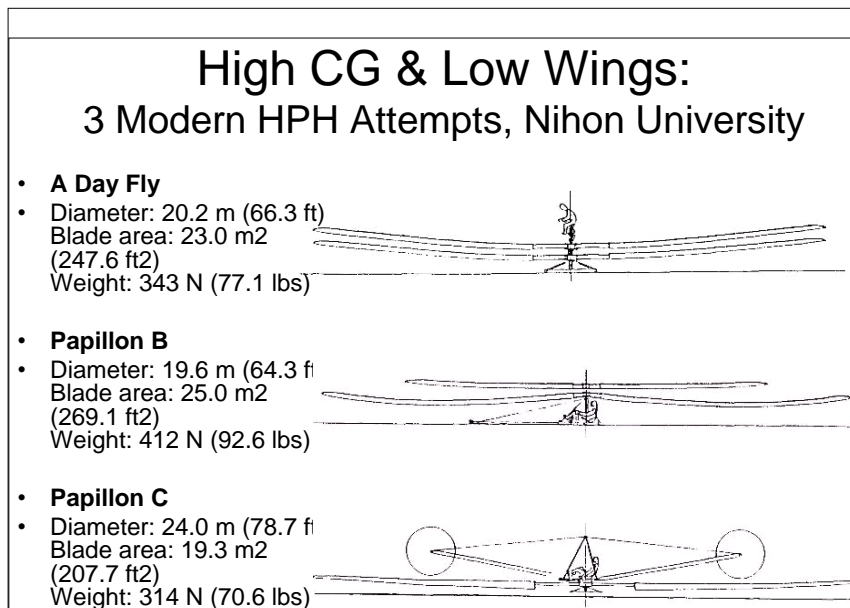
Figure 1-6 Examples of Low Rotor/Higher Center of Gravity HPH Designs (Sopher 1997)

6

This type of low rotor configuration is naturally unstable because the higher CG needs to be actively balanced and continually corrected by the pilot. However, during an HPH flight attempt, the pilot would be so physically engaged in exerting peak power for his/her 60 second sprint, that such active piloting would be a considerable distraction.

- *Coaxial Interference.* On coaxial counter-rotating systems, aerodynamic buffeting and physical collisions typically occur because the two systems are too close together. Close overlay of coaxial systems further precludes wire bracing for the upper rotor system. (Furton 2004)

Figure 1-7 Example of Coaxial Rotor Physical Interference, Thunderbird (Human 2008)

1.2 Purpose of the Study

This thesis proposes a rotor system concept for an HPH that would be sufficiently lightweight so as to be built large enough to satisfy the prohibitive design constraints warranted by such an aircraft.

Thesis: A wire-braced semi-rigid rotor system, positioned well above the pilot and with sufficient offset between the two rotor discs, could be built large enough to

support the enormous rotor diameter required for a potentially successful HPH, and yet still be sufficiently lightweight to meet the marginal power available and also be strong enough to control rotor geometry and efficiently generate lift. See Figure 1-8 for a graphical rendition of the thesis statement.
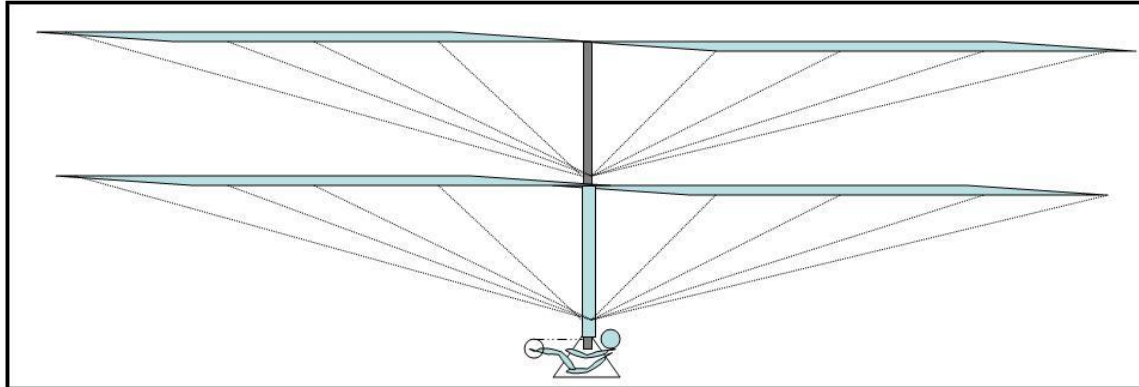
Figure 1-8 Proposed Concept for a Wire-braced Semi-rigid Coaxial Counter-rotating HPH

A series of concept demonstration models, scaled in both size and power, would validate the design.

1.3   Significance of the Study

The designing, building, and ultimate sustained flying of a successful HPH would be a remarkable milestone in human discovery and in aviation. It will require the synthesis of innovative engineering, best practices in modern manufacturing, and the utmost in human physical performance. Large, ultra-light rotors will be the key to such an achievement. This thesis is supported by a series of interlocking hypotheses that might make such a rotor system attainable.

1.4   Hypotheses

The following hypotheses were tested in this thesis:

1.4.1   Hypothesis 1

A large, elevated, wire-braced rotor system could be built sufficiently lightweight to support the design of an ideal HPH because external bracing wires would bear the majority of the airfoils' lifting loads, greatly reducing the rotors' structural design requirements and their consequent weight. Such a wire-braced semi-rigid structure could be as much as five (5) times lighter than a comparable rigid airfoil.

1.4.2   Hypothesis 2

Wire-braced wings would prevent rotor coning and the associated loss of lift. Rigged to appropriate lengths, the bracing wires could keep the rotor system completely parallel to the ground.

1.4.3   Hypothesis 3

Wire-bracing of the semi-rigid airfoil would additionally control the twisting and pitching angles of the rotor, and thus enable the otherwise prohibitive geometries of such a lightweight airfoil. In a static condition, the semi-rigid airfoil would droop and twist; however, in powered rotation, the lifting airfoil would rise until stopped by the bracing wires. Connected to both the leading and trailing sections of the rotor, the bracing wires could be rigged so as to control the twisting of the airfoil and to enable desired angles of attack all along the rotor.

1.4.4 Hypothesis 4

The significant offset between rotor diameters, necessary for the wire-bracing of the upper rotor system, would prevent physical interference of the two rotor discs.

1.4.5 Hypothesis 5

The wire-braced offset elevated coaxial counter-rotating rotor system could generate enough necessary lift to achieve hovering flight.

1.4.6 Hypothesis 6

An elevated rotor system would be inherently stable because it would place the relatively heavy pilot-engine far below the center of lift and, therefore, create pendular stability.

1.4.7 Hypothesis 7

The aerodynamic drag and consequent power penalty caused by the external bracing wires would be more than offset by the power saved through the reduced weight of the rotors afforded by the bracing wires.

1.5 Delimitations

The purpose of this thesis was to prove a particular concept, not to provide a detailed, optimized design for either the scale models or for a potential full-size HPH. Therefore, the following factors, design components, and conditions are identified as variables that were either outside the scope of this study or that were not statistically evaluated as significant contributors toward the final analysis:

10

1. Full scale HPH design details

2. Efficiency of drive system to the coaxial masts

3. Optimization of Rotor Geometry, Dynamics, and Aerodynamics

2 Background and Review of Literature

The history of human-powered flight has evolved from ancient legends, such as the wax-fastened wings of Greek architect Daedalus and his son Icarus, to the practical and innovative fifteenth century sketches of Leonardo da Vinci, onto numerous modern scientific pursuits of both human-powered airplanes and helicopters (Taylor 1995)

This chapter provides a literature review of the history of the human-powered flight, first reviewing the success of human-powered fixed-wing airplanes and then the progress being made with human powered helicopters.

2.1 History of Human-powered Airplanes

Beyond merely jumping, falling, and/or gliding, serious efforts for human-powered flight began to escalate in the early nineteen hundreds—soon after the Wright brothers flight at Kitty Hawk had ushered in the age of powered flight. Engine powered aircraft were being developed for ever broadening applications and ever increasing performance. And while human-powered vehicles did not have any foreseeable practical applications, incentives for their development often came to the would-be builder in the form of competitive prizes, sponsored by curious and adventurous philanthropists.

2.1.1   Early Prizes and First Flights

Two of the first such prizes were sponsored in France by Robert Peugeot for flights of one, then later, ten meters. These were both won by Gabriel Poulain on his custom made bicycles with overhead wings (see Figure 2-1). To fly, he would pedal his cycle to build up speed on the ground; then, at peak velocity, would pull a lever to snap the wings into their six degree up angle and lift off—flight! (Grosser 1991)
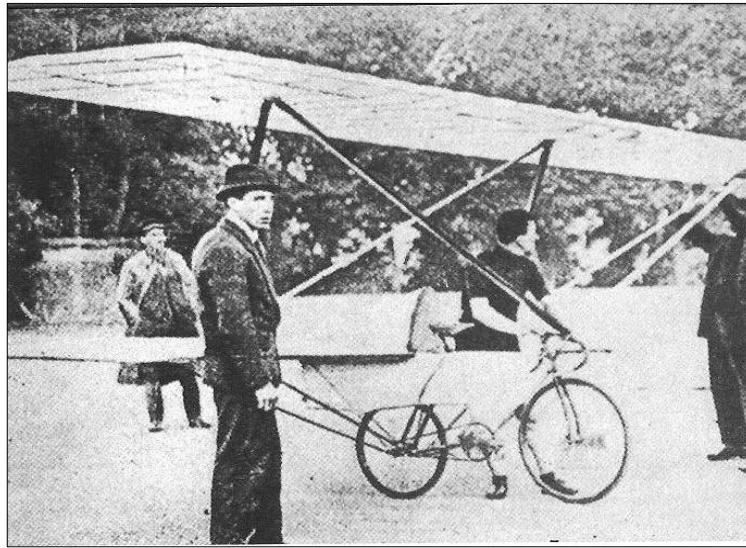
Figure 2-1 Gabriel Poulain's Flying Bicycle (Grosser 1991)

Sustained flight, however, would require more than a bicycler's inertia; some source of airborne thrust would be required, such as a propeller. This lead to additional prizes for even longer distances.

While additional prizes and records were won in the 1920s and 30s, much of the enthusiasm of human-powered flight was overcome by the first and then second world wars. Even after the wars, most of the aerodynamic community was so focused on developments of bigger and faster aircraft that serious efforts for human-powered flying

didn't resurface until the 1950's. These were seen first by an occasional scholarly article on the subject and then in 1957 with the formation of the Man-Powered Aircraft Committee (MANPAC) at the College of Aeronautics at Cranfield, England. While MANPAC did well a promoting the feasibility and scientific merits of human-powered flight, it wasn't until they enlisted the financial backing of Henry Kremer in 1959 to sponsor a new prize. (Grosser 1991)

2.1.2   The Kremer Prize

The Kremer Prize was established, five thousand pounds (approximately $14,000 at the time) to the first person who could meet a series of milestones in a single flight to prove both sustainability and controllability. Key requirements of the Kremer Prize are as follows:

1. The aircraft must be a heavier-than-air machine (no balloons), powered and controlled entirely by its pilot

2. The aircraft must take off from level ground in still air entirely by human power.

3. The aircraft must fly a figure-eight course with two turning points not less than one-half mile (0.8 km) apart.

4. The aircraft must fly over a 10-foot (3 m) altitude marker at the starting line and cross the same marker again at the finish line.

Through the 1960s and 70s several remarkable aircraft took to the air, both in Europe and the U.S. but none could combine controllability and endurance. The aircraft that flew the furthest could only do so in a straight line. And those that seemed better at turning couldn't go the distance. (Grosser 1991)

2.1.3   The Gossamer Condor

The Kremer Prize was finally won on August 23, 1977 by a team lead by Dr. Paul MacCready. His *Gossamer Condor* was a case study in simple, rugged, minimalistic design. He deliberately chose to use aluminum tubing instead of lighter weight advanced composites because of aluminum's ease of availability, manufacturability, and reparability. The Condor could crash and crumple—looking totally demolished and yet be fixed up and ready to fly later the same day (see Figure 2-2). Weight optimization of components was brutal and effective—if a part hadn't broken yet, it was too heavy, so material would be removed (often via a drill bit) until it was just barely strong enough. Their motto was, "Do only what you have to, and build quick and dirty." (Grosser1991)

Figure 2-2 Paul MacCready's Gossamer Condor HPA in Flight (Grosser 1991)

After the Gossamer Condor, MacCready and many others continued to build ever more efficient airplanes, achieving ever longer flights. Controlled, sustained human-powered flight had been achieved and mastered.

2.2 History of Human-powered Helicopters

Attempts to take off vertically (without a runway) and then hover via a human-powered helicopter (HPH), however, haven't yet shared the same degree of success as have their fixed-wing counterparts.

In 1980, the American Helicopter Society (AHS) established a new prize, modeled after the success of the Kremer Prize, to encourage the development of a successful human-powered helicopter (HPH). Named in honor of Igor Ivan Sikorsky, the father of modern helicopters, the Sikorsky Prize will award $20,000 to the first HPH that can demonstrate both sustainability and controllability by achieving the following contest requirements all during a single flight:

- **Duration**: Hover for one minute (60 seconds)

- **Altitude**: The lowest part of the aircraft must reach a momentary altitude of 3 meters during the 60-second flight

- **Controllability**: Remain within a ten meter zone; pilot may not spin (Sopher 1997)

2.2.1 The Da Vinci III

Of the dozens of attempts, two HPH's have actually flown, albeit briefly and very low to the ground.

The first HPH to lift off was built by students at California Polytechnic State University. Their *Da Vinci III,* as shown in Figures 2-3 and 2-4, with its 100-foot rotor and dual tip-drive propellers made a single flight in 1989 that lasted for 7.1 seconds and reached an altitude of 8 inches. (Drees 1993)
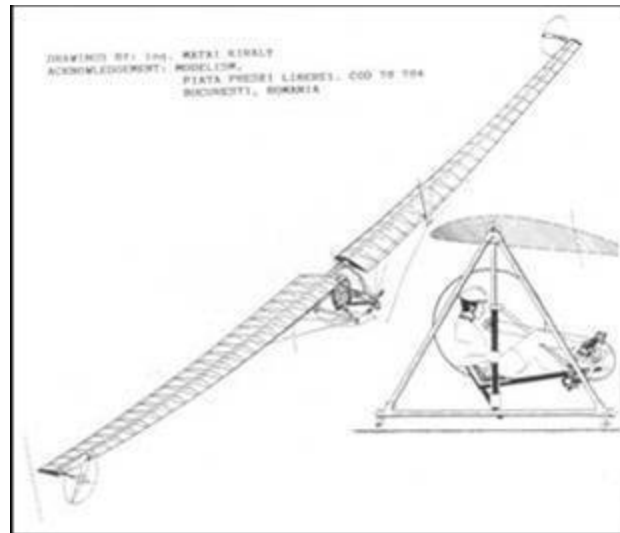
Figure 2-3 Schematic of the Da Vinci III (Cal 2008)

Figure 2-4 Cal Poly's "Da Vinci III"Achieving Inches of Flight (Cal 2008)

2.2.2 The Yuri I

The second and only other HPH to ever fly was designed by Akira Naito, a former professor from Japan's Nihon University. Naito lead design teams on several different HPH attempts in the 1980s and '90s, some of which were depicted earlier in Figure 1-3. Their first and only aircraft to ever fly was his quadrotor Yuri I (see Figure 2-5). In March of 1994, the Yuri I flew for 19.46 seconds to a momentary altitude of eight inches. (Drees 1995)

Figure 2-5 Yuri 2 in Flight (Human 2008)

2.3 Conclusion

Human-power has proven to be a sufficient power source for human powered flight, particularly in human-powered airplanes and with limited, encouraging success for helicopters. Some progress has been made toward vertical liftoff and a controlled, sustained human-powered hovering flight.

3 Methodology

In this chapter, key features of a nominal full scale wire-braced semi-rigid elevated rotor system for a conceptual HPH are first outlined and defined. Then, in order to test the seven hypotheses of this thesis, a series of experiments are designed to be conducted using both physical and analytical models. Next, a series of proof-of-concept scale models ranging in functionality and complexity were designed in order to support the proposed experiments. Finally, an analytical model was developed to test the seventh hypothesis concerning the power required to overcome the aerodynamic drag induced by the bracing wires.

3.1 Nominal Full-size Design

The general design of the conceived HPH with its proposed wire-braced semi-rigid elevated rotor system is illustrated in Figures 3-1 and 3-2. Key features include:

- Large Rotors

- Ultra-lightweight and Flexible Rotors

- Two Coaxial Counter-rotating Rotor Systems

- Elevated Rotor Systems

- Wire Braced Rotors

- Low Pilot-Engine
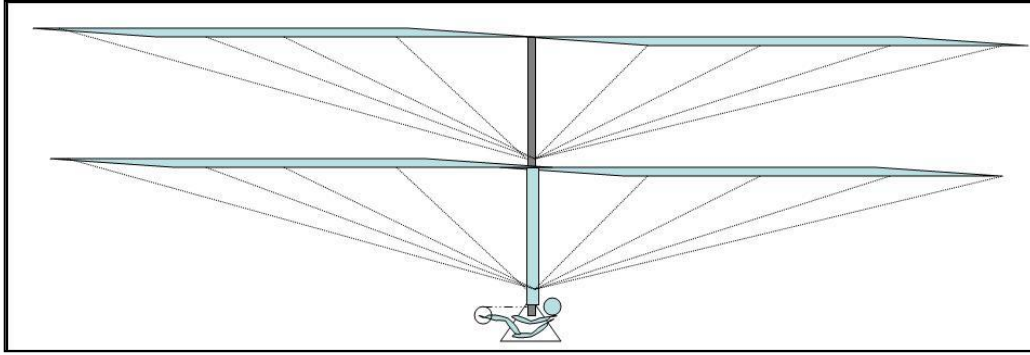
Figure 3-1 Proposed Concept for a Wire-braced Semi-rigid Coaxial Counter-rotating HPH
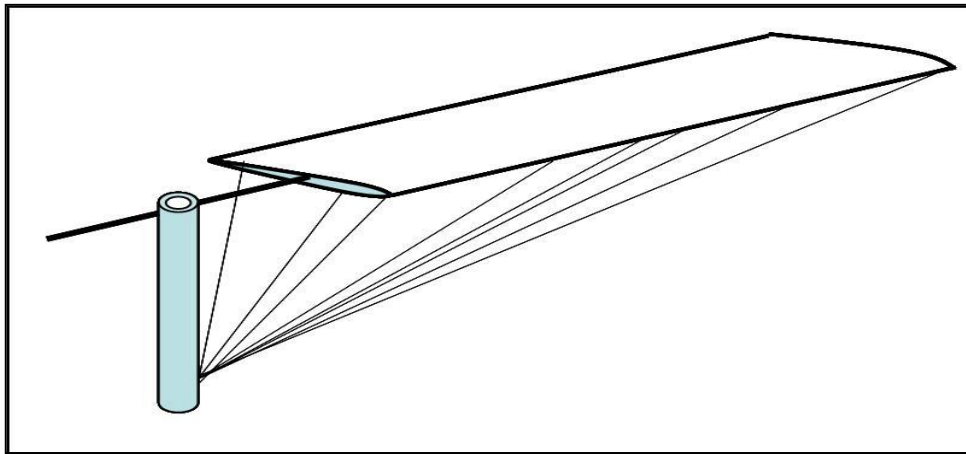
Figure 3-2 Semi-rigid Wire-braced Elevated Rotor Concept

The following sections define the key parameters of a nominal full-scale wire-braced elevated coaxial rotor system for a human-powered helicopter. Key features to be defined are:

1.   Rotor diameter

2.   Rotor heights

3.   Target weight of rotors

3.1.1　Rotor Diameter

Requisite rotor diameter is a function of power available and thrust required (for a helicopter to hover, thrust must be at least equal to total weight: aircraft + pilot). Multiple design studies have been performed on the feasibility of an ideal HPH and, though their outcomes vary, the more conservative of these studies consider a configuration driven by a single pilot of estimated weight 650N (approximately 65 kg of force) and an empty aircraft weight of 350N (approximately 35kg of force). When calculating for a single plane rotor system, a resulting diameter of 35m is required. (Filippone 2002)

Single plane rotor diameter = 35m　　　　　　　　　　　　　　　　　　　　**(3-1)**

3.1.2　Coaxial Rotor Diameter

The concept rotor system proposed in this thesis is a coaxial counter-rotating rotor system type. Coaxial rotor systems are considered to have 1.5 effective disc areas compared to a single plane rotor system. Therefore, the requisite 35m rotor diameter could be effectively substituted with two coaxial 23.3m diameter rotor systems. (Cranfield 1987)

$$\text{Coaxial Rotor Diameter} = \frac{SinglePlaneRotorDiameter}{CoaxialFactor} = \frac{35m}{1.5} = 23.3m \qquad \textbf{(3-2)}$$

Consequently, each individual rotor would have a span of half the total rotor diameter:

$$\text{Single Rotor Length} = \frac{Diameter}{2} = \frac{23.3m}{2} = 11.7m \qquad \textbf{(3-3)}$$

3.1.3 Rotor Heights

The two rotor systems need to be elevated to a sufficiently high offset of each other to enable effective wire bracing, to provide sufficient offset between the two rotor systems, and to provide a high-enough center of lift to enable the inherent pendulum stability of the relatively low center of gravity. This assumes the relatively heavy pilot would be at the very bottom of the structure. Based on the height-to-wingspan ratios of the wire-braced wings on successful human-powered airplanes, such as the record setting Gossamer Condor and the Gossamer Albatross, a nominal ratio of 1:4 was observed. (Burke 1980) Therefore the height of each plane would need to be:

$$\text{Height of Rotor Plane} = \frac{RotorRadius}{Height:WingspanFactor} = \frac{11.7m}{4} = 2.9m \qquad \textbf{(3-4)}$$

3.1.4 Nominal Design Summary

The following table outlines the key design features of a nominal wire-braced coaxial rotor system:

Table 3-1 Nominal Design Summary

Design Feature	Estimated Dimension
Rotor Diameters: Coaxial Two-plane System	23.3m
Individual Rotor Lengths	11.7m
Rotor Heights	2.9m
Structure Weight	350N (approximately 35 kg of force)

3.2   Scale Model Designs

An appropriate scale factor was needed in order to build the concept demonstrator models of sufficient size sufficient to test the hypotheses, yet still small enough to be built and tested in an indoor laboratory environment. A factor of 1:10 scale was used in the design of all three models. Based on the nominal parameters discussed previously, the following 1:10 scale parameters were calculated:

Table 3-2 Design Summary: Nominal and 1:10 Scale

Design Feature	Nominal, Full Scale	1:10 Scale
Rotor Diameters: Coaxial Two-plane System	23.3m	2.33m
Rotor Lengths	11.7m	1.17m
Rotor Heights	2.9m	0.29m
Structure Weight	350 N	0.35 N(approx 35g of force)

The primary and common component of all the models is the semi-rigid airfoil for the wire-braced rotor.

3.2.1   Airfoil Chord Selection

At very low Reynolds numbers (the product of small airfoils at low air speeds; abbreviated Re), the best airfoils are typically very thin, more of an arc than a conventional teardrop. (Raskin)

The 1:10 scale mode airfoils to be designed would have an estimated Re of approximately: 20,000 to 30,000

$$Re = (\text{speed in m/sec})(\text{chord in cm})(680) = (2 \text{ to } 3 \text{ m/s})(14\text{cm})(680) \qquad \textbf{(3-5)}$$

Re = approximately 20,000 to 30,000

The basic rotor shape for the models was patterned after the AS6074 Constant Chord, 17% semi-symmetrical airfoil, made from expanded polystyrene. While the AS6074 airfoil is notably thicker than most lower Reynolds number airfoils, only its upper surface was to be used, thus creating an arc airfoil.

3.2.2   Single Airfoil Weight Model

The first and simplest model would be a single rotor, built to 1:10 scale to test Hypothesis 1: Sufficiently Lightweight.

3.2.3   Single Airfoil Geometry Model

The second model would be operated manually and would test Hypothesis 2 *Prevent coning*; and Hypothesis 3 *Control airfoil geometry/pitching angle of attack.* These tests could be performed using brief, two to three second sweeping test passes at

desired rotational velocity in order to observe the rotor in a lifting flight profile. The model would be comprised of a single wing, mounted to a mast and wire-braced.

3.2.4   Non-flying Single-plane Model

This third model would further test Hypotheses 2 and 3 in a continuous rotational condition, rather than just short sweeping passes. This model would require two counterclockwise wings to be mounted to the mast and would be driven by a DC electric motor while mounted to a static test stand.

3.2.5   Flight Test/Lifting Force Model

This fourth and most complex model would be a fully functioning coaxial dual-plane wire-braced dual-rotor-system air vehicle, driven by a dc motor powered with its own integrated battery pack. This model would test Hypothesis 4 *High Rotors with Sufficient Offset to Avoid Interference*, Hypothesis 5 *Sufficient Lift*, and Hypothesis 6 *Inherent Pendular Stability*.

This model would require two coaxial masts. The outer mast would need to be a hollow tube with a sufficient inner diameter to accommodate the free spinning inner mast; it would also need to be at least 29 cm tall. The inner mast would need to fit freely within the outer, lower mast and would also need to be twice as tall.

In order to test the operation of this model prior to its first free flight excursions, a dynamic test stand would be necessary, one that would need to provide pitching and rolling stability yet still allow full rotation and vertical movement under lifting conditions.

27

3.2.6 DC Motor and Gearhead Requirements

The nominal full-scale design was based on power generated by a world-class cyclist to the order of 600W to 1000W during the required one-minute flight. At 1:10 scale, the model would only have one-one-thousandth the weight of its full-sized counterpart:

$$\text{Scaled Weight} = \text{Scale Factor Cubed} = \left(\frac{1}{10}\right)^3 = \frac{1}{1000} \qquad (3\text{-}6)$$

Thus, the motor required to power the coaxial model would need to have a maximum output shaft power of only 1W to lift the 100+g aircraft.

The motor would also need to be limited to an RPM that could support an intended blade tip speed of around 3 meters per second for each respective rotor system. For the 1:10 scale model, the circumference is approximately 7.3m; thus the needed rpm is calculated as follows:

$$rpm\frac{rpm}{CoaxialSplit}\left(\frac{1\min}{60\sec}\right)circumfrence = DesiredTipSpeed \qquad (3\text{-}7)$$

The Coaxial Split divides the nominal motor rpm by 2, since the motor housing itself is a rotating component in the opposite direction of the motor rotor. Allowed to spin freely, and driving equivalent loads, both the rotor and the housing would spin in opposite directions at half the rpm of the motor rotor alone; therefore:

$$\frac{rpm}{2}\left(\frac{1\min}{60\sec}\right)7.3m = \frac{3m}{s} \qquad\qquad \textbf{(3-8)}$$

Solving for rpm:

$$rpm = \frac{\left(\frac{3m}{s}\right)(2)(60\sec)}{7.3m} = 50 \qquad\qquad \textbf{(3-9)}$$

Thus, the motor's target rotational speed should be approximately 50 rpm.

Most DC motors in this power class, however, have much higher speeds, typically around 10,000 rpm. Therefore, the motor output speed would need to be geared down to the approximate range.

3.2.7   DC Motor and Gearhead Selection

In order to get the estimated 1W of power from a DC electric motor, turning at the much slower required speed, a customized motor and inline mating gearhead were procured (see Figure 3-3). The motor would need to have sufficient power above the desired 1W to account for motor efficiency losses, then gearhead efficiency losses.

Power Available = (Motor Power)(Motor Efficiency)(Gearbox Efficiency)   **(3-10)**

A Faulhaber series 1331 006SR DC-Micromotor, rated for 3.11W at 81 percent efficiency, was selected. A mating inline Faulhaber 14/1 Series Planetary Gearhead with

a reduction ratio of 134:1 was then selected, with an efficiency of 60 percent. Both the micromotor and the inline gearhead are depicted in Figure 3-3.
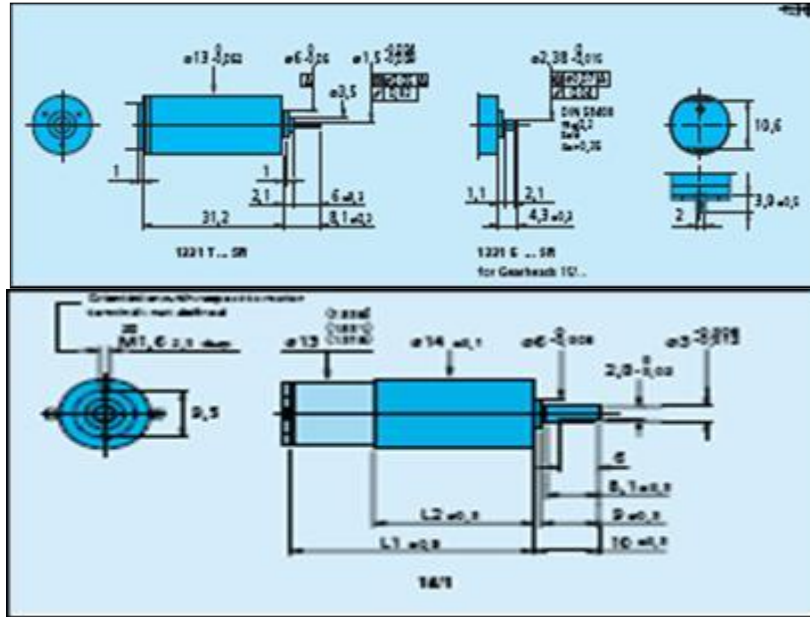
Figure 3-3 Faulhaber DC Micromotor & Inline Gearhead (Faulhaber 2008)

Therefore, total usable power from the micromotor and gearhead is shown in Equation 3-10.

Power Available = (3.11W)(.81)(.60) = 1.51 W   **(3-11)**

3.3   Analytical Model for Wire Drag

Hypothesis Seven proposed that the sum of all the drag induced by the bracing wires would incur a smaller power penalty than the power saved, thanks to the structural weight-savings benefit afforded by the wires. In order to prove this hypothesis, the drag of each wire would first need to be understood.

The drag of any object is a function of its shape, size, and speed moving through a medium of known density. Since all these variables would be known for the scale model HPH, an analytical model could be used based on established aerodynamic and fluid dynamic principles.

The drag formula is as follows, where D = drag, ρ= the density of the air, V is the velocity of the object, Cd is the Coefficient of Drag, and S is the surface area of the wire.

$$D = \frac{1}{2}\rho V^2 C_d S \qquad\qquad\qquad \textbf{(3-12)}$$

The Cd component of Eq. 3-11 depends on the objects shape and corresponding Reynolds number. For Cylinders the Cd is described in Figure 3-4. (Munson 1993)
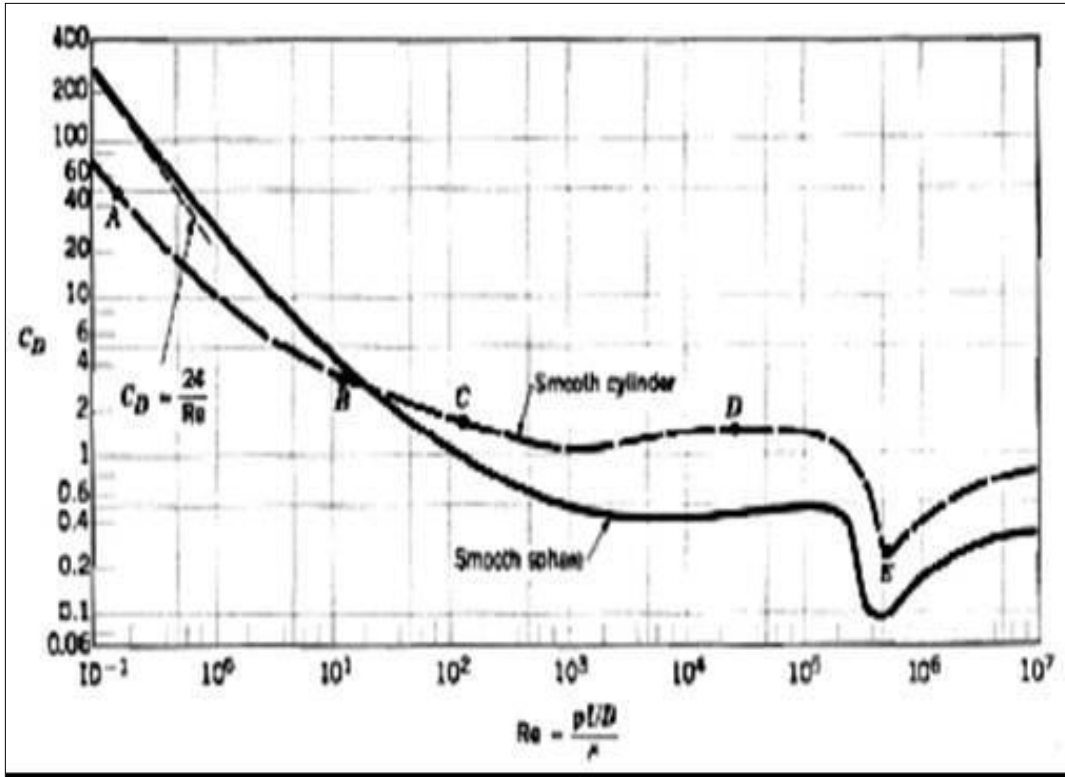
Figure 3-4 Drag Coefficient as a function of Reynolds number for a Smooth Cylinder (Munson 1993)

The aerodynamic Reynolds number (Re) is a function of air density, velocity, reference size/area of the airfoil, and air viscosity.

$$\text{Re} = \frac{\rho U D}{\mu}$$

(3-13)

Because velocity is variable to both Cd and to Re, and since the tangential velocity of a rotating object at a given rotational speed, Omega (Ω) varies depending its arc length (zero tangential speed at the hub and maximum speed at the tip), a formulaic relationship was established between Cd and Re.

Using Figure 3-4 to determine several reference data points of Cd for a given Re, a graphical relationship was plotted and a trendline was drawn to estimate the approximate relationship between Cd and velocity. The equation of the trendline was also approximated. See Figure 3-5.

Drag Coefficient

$y = 4.0091x^{-0.4268}$
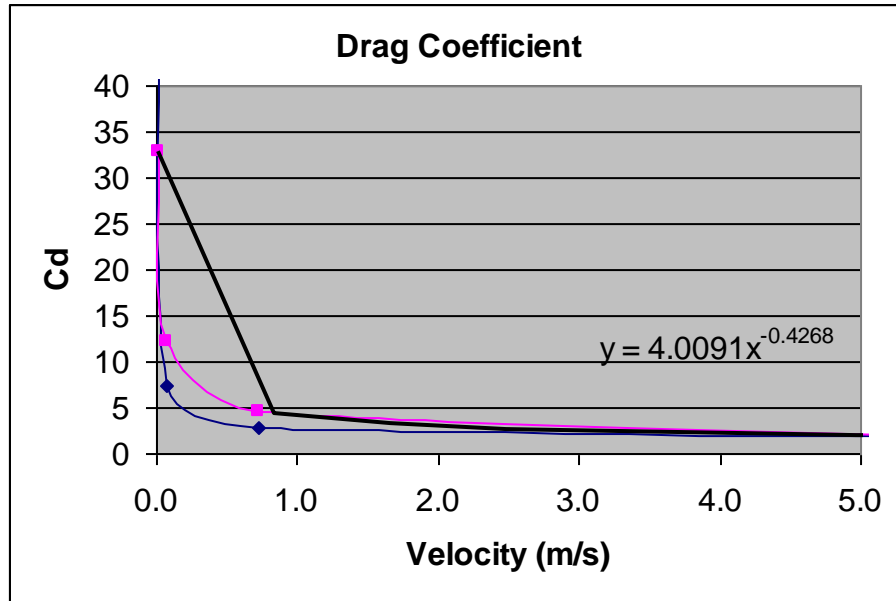
Figure 3-5 Approximated Relationship of Coefficient of Drag to Velocity

The result was used to provide an approximate relationship of Cd as a function of Velocity (U):

$$Cd \approx 4.0091.9U^{-0.4268} \tag{3-14}$$

The drag on each wire as a whole needed to be considered as the sum of all the drag on the wire, which constantly varies depending its radial length. Therefore an analytical approach was taken to mathematically divide the individual wires into

theoretical 1cm long segments—each theoretically perpendicular to the axis of rotation—

and then sequentially derive the following metrics for each wire segment:

1.   **Radial length** in meters: r = distance to hub

2.   **Tangential Speed** in meters per second: $U = r\,\Omega$

3.   **Coefficient of Drag**: Cd approximated by Eq. 3-15

4.   **Drag** in Newtons: D per Eq. 3-16

5.   **Torque** in Newton meters: $\tau = rD$

6.   **Power required** to move each wire segment in Watts: $W = \tau\,\Omega$

7.   **Factored Power required** to move each segment: Factored increase to account for each segment's actual (longer) length: hypotenuse of each 1cm segment

8.   **Total of Power required per wire**: Sum of all segmental power required, depending on the length of the wires.

See Chapter 6 for detailed analysis and results of the drag experienced on each wire and the total drag induced by all the bracing wires.

4 Building the Models

After each proof of concept model was designed and necessary materials were procured, the models were built. This chapter documents the build of the four (4) models.

4.1 Cutting the Foam Ribs

Using a hot wire cutter, the AS6074 airfoil was cut into sections approximately 3.5mm thick, as shown in Figure 4-1. These sections would become the models' ribs.
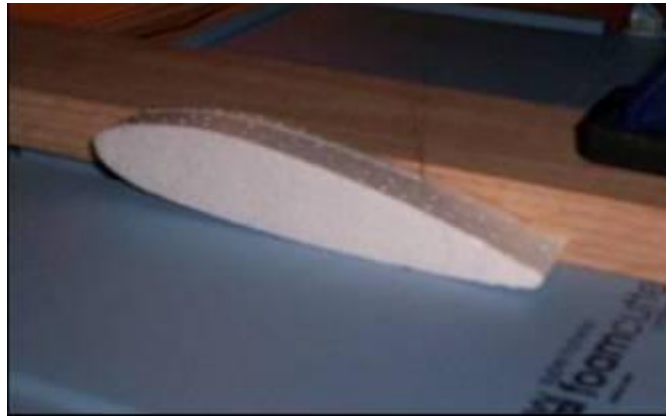
Figure 4-1 Hotwire Foam Cutting of Rotor Ribs

Notches were also wire cut at the leading edge and trailing edge to accommodate the two spars shown in Figure 4-2.

Figure 4-2 Cutting the Leading Edge Spar Notch in a Stack of Four Ribs

Lastly, two 3.2mm tooling holes were drilled in each rib along its centerline at 22mm and 100mm from the leading edge, to enable set-up in the assembly fixture.

4.2 Assembly Fixture

A herringbone fixture was created to hold the ribs in place while each was glued to the leading edge spar and the trailing edge spar as shown in Figure 4-3

Figure 4-3 Herringbone Fixture: Bonding Ribs and Spars

Spacer blocks were fabricated and used to separate each rib by approximately 89mm during the bonding process.

4.3   Airfoil Covering Application

After each rib was securely fastened to its leading and trailing edges, the herringbone fixture was slid out of each airfoil framework. The structure was then ready to have its skin covering applied. The covering material selected for use was 21st Century® Coverite ™ Microlite ™, the lightest iron-on covering available. This thin film was first cut to an oversized dimension and lightly laid upon the framework. Then, using a modeling sealing iron, heated to about 90°C, the film was firmly applied to the leading and trailing edges and the top of each rib as shown in Figure 4-4.

Figure 4-4 Hot Iron Application of Microfilm

After the film was completely applied, the iron temperature was increased to approximately 110°C to tighten the heat-shrinking film. Finally, the excess material was trimmed from all edges.

4.4   Wire Bracing: Initial application

The nylon bracing wires were then tied to the tooling holes on the first, fourth, seventh, and tenth ribs as shown in Figure 4-5. The wires were cut oversized to support later rigging.

Figure 4-5 Attachment of Bracing Wires to Foam Ribs

4.5   Mast and Integrated Hub

Three mast-and-hub assemblies were then created. For the masts of the single rotor system models and for the inner mast of the coaxial model, a 3.5mm carbon fiber solid rod was selected. For the outer mast of the coaxial model, a carbon fiber tube with 6.1mm outer diameter and 3.6mm inner diameter was selected.

The rotor hubs were permanently attached to the top of each mast. The hubs were composed of two 15mm by 15mm by 25mm foam blocks that supported two 130 mm long thin walled aluminum tubes, each with an inner diameter of 3.00mm. The entire assembly was secured to the mast using a two-part thermoset epoxy. (See Figure 4-6)
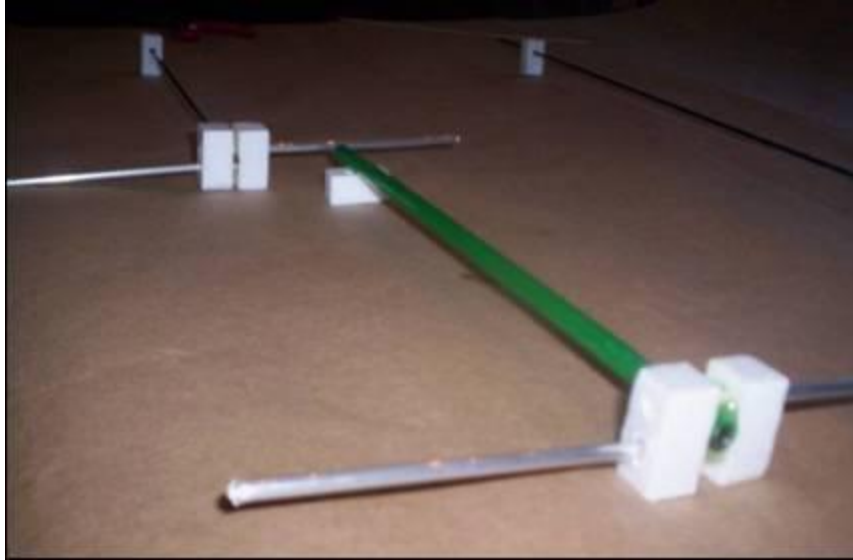
Figure 4-6 Mast and Hub Assemblies

4.6   Rigging

The rigging of each rotor to the mast was accomplished by first inserting the dowel root of each rotor into the corresponding thin-walled aluminum sleeve of each hub; the fit was snug enough to allow minor adjustments of the rotor's pitch angle. Once the desired pitch angle was achieved, the dowel-sleeve union was wrapped with a single strip of tape to secure the fit. The entire assembly was then turned upside down so the rotors would be flat along the work surface and the mast would be vertical. The nylon wires were then pulled up to their attachment points on the masts and locked into place with a strip of masking tape. (See Figure 4-7)
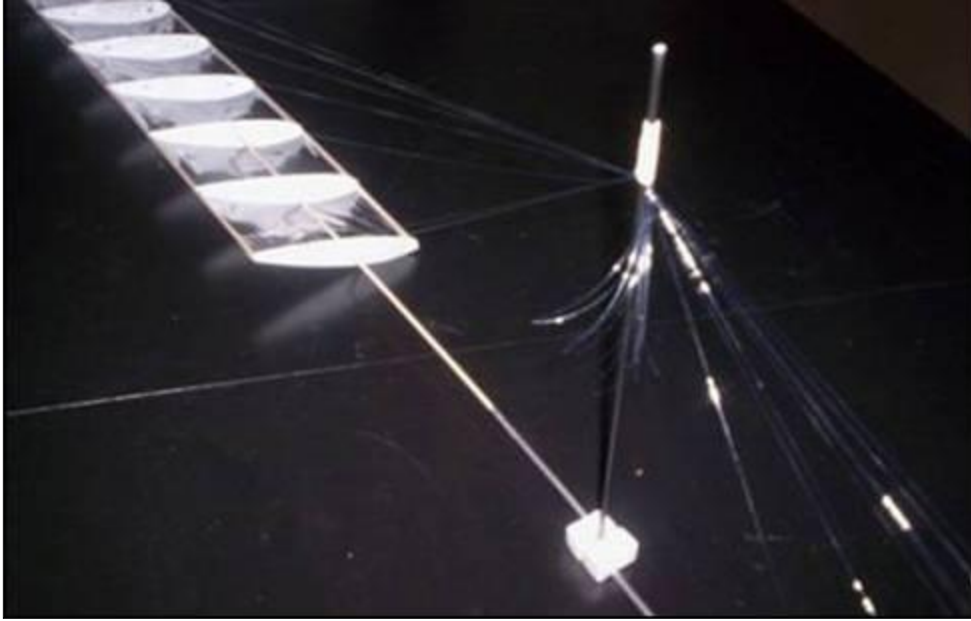
Figure 4-7 Rigging the Rotor System: Nylon Wires Pulled then Locked into Position

4.7 Coaxial Assembly and Motor Attachment

With both rotor systems rigged to their respective masts, the two were ready to be assembled and attached to the drive motor, as shown in Figure 4-8.
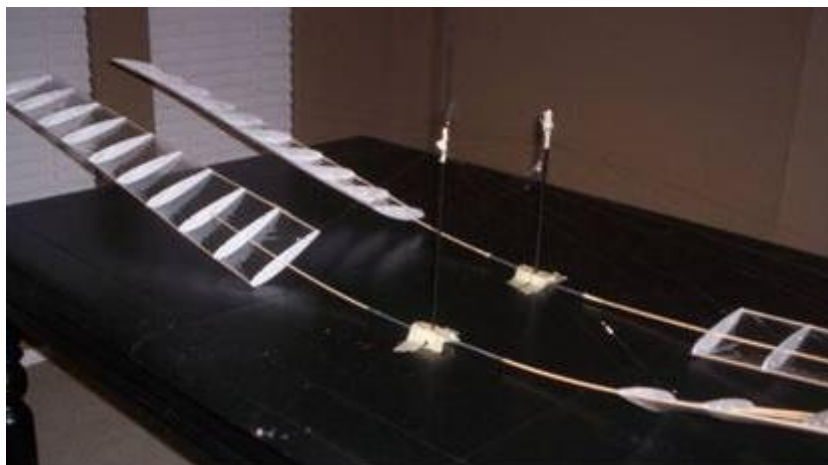
Figure 4-8 Upper and Lower Rotor Systems

The inner mast (upper rotor system) was slid smoothly into the outer mast (lower rotor system). The lower end of the inner mast was then coupled to the motor's output rotor via the gearhead coupling. Next, the outer mast (lower rotor system) was attached to the motor/gearhead housing via a drive collar that was designed to fit freely around the gearhead coupling. Finally, the 6V power supply and the switch were attached to the motor. (See Figure 4-9)
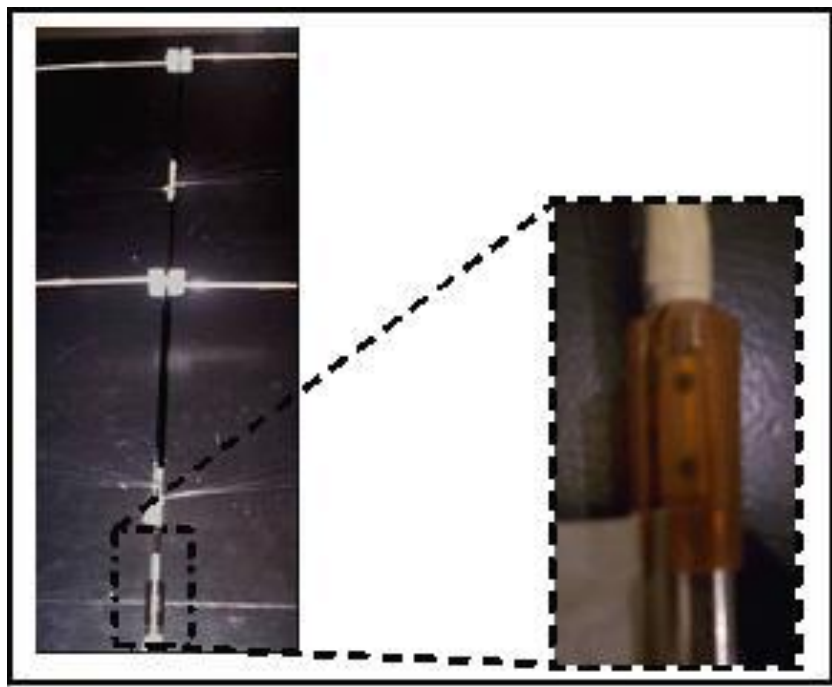
Figure 4-9 Coaxial Mast Assembly (Left) and Torque Collar (Right)

5 Functional Testing of the Models and Test Equipment

After the models were built, the basic functionality of each model and the respective test hardware were verified to ensure that they would each operate suitably for their respective performance testing.

5.1 Flexibility of Semi-rigid Rotors

Both spanwise bending/coning and twisting flexibility were easily manifest with only gentle manual manipulation as shown in Figures 5-1 and 5-2.

Figure 5-1 Spanwise Bending "Coning" Demo
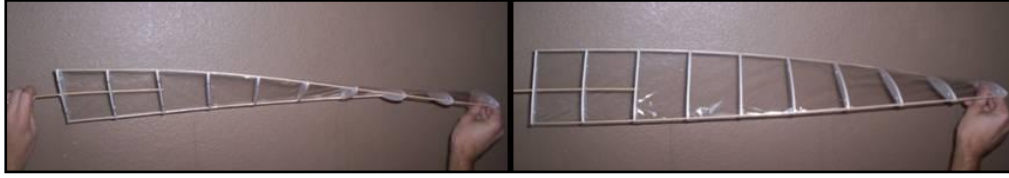
Figure 5-2 Twisting Flexibility Demo: Pitching Down (Left) and Pitch Up (Right)

5.2   Test Stands

While some performance tests could be conducted without test stands, others required some means of restricting certain degrees of freedom of the models, depending on the tests to be conducted. Two test stands were prepared and checked for functionality.

5.2.1   Static Whirl Stand

This stand was to be used for the observation and measurement of the wire-braced rotors using only the single plane model. It required a solid mounting base in which to rigidly seat the motor. Under a test run, the stand proved fully functional and the rotation was stable, as shown in Figure 5-3.
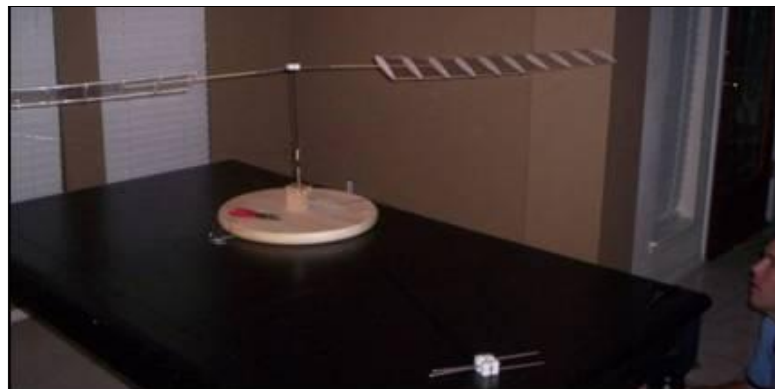
Figure 5-3 Single Plane Model Loaded in the Static Whirl Stand

5.2.2   Dynamic Test Stand

The intent of the dynamic test stand was to hold the coaxial model in a vertical position during "lifting force" tests, yet still allow the model to spin freely, to bear its own weight (being measured on a scale beneath the model) and to be lifted freely off the scale during performance test runs to measure the lifting forces.

The dynamic test stand was tested to ensure that it would allow the motor/gearhead to fit smoothly into the guide channel and to keep the model vertical without bearing any of its weight or restricting the ability of the models to rotate. With just the motor and gearhead it appeared to be fully functional, allowing free rotation. (See Figure 5-4)

Figure 5-4 DC Power Supply and Motor/Gearhead

By applying a range of input voltages to the motor, measurements of the resultant rotational velocities produced by at gearhead drive shaft were measured. (See Table 5-1)

Table 5-1 DC Motor and Gearhead Functional Check: RPMs for given Voltages

Input Voltage	Observed Rotations During 10 second Interval	Measured RPM = (observed results) times 6
1.5V	3	18
3.0V	6.5	39
6.0V	13	78

The observed 6V result of 78 rpm was very close to the estimated nominal output of approximately 79.1 rpm, based on the factory specified 10,600 rpm slowed by the 134:1 inline gearhead.

6 Performance Results

Using the assembled rotors, test hardware, and analytical models, each hypothesis was tested to measure its degree of validity.

6.1 Lightweight Airfoil Test

The first hypothesis proposed that a wire-braced semi-rigid rotor would be up to five times lighter weight than a comparable rigid airfoil. In order to test this theory, the completed rotor's surface area and weight were first measured, as shown in Figure 6-1.

Figure 6-1 Test to Weight the Semi-rigid Rotor

6.2 Weight and Surface Area Results

As built and tested for this thesis, the basic semi-rigid rotor weighed 9.1g with a total surface area of 0.12m; its resultant weight-to-surface area ratio was 78.3g/m². In Table 6-1, these results were compared to comparable lightweight rigid wings and rotors, including:

- The solid foam counterpart to the semi-rigid model (AS6074)

- Three ultralight indoor flying rubber band model (Gitlow 1993)

- Five full-sized HPH rotors (Sopher 1997 and Gavaghan 1989).

In order to compare the results in an equitable manner (since *volume/weight* are a cubed function while *area* is only a squared function) the final weight-surface area numbers for each airfoil needed to be normalized according to their scale factor to the thee halves power relative to the models built and tested in this thesis.

Table 6-1Comparison of Normalized Weight-to-Surface Area Ratios

Airfoil	Type	Weight (g)	Surface Area (m^2)	Weight-to-Surface Area (g/m^2)	Relative Scale	Scale to the 3/2 power	Normalized Weight-to-Surface Area (g/m^2)
Wire-braced Semi-rigid (WBSR)	Model Rotor from this Thesis	9.1	0.12	78.3	1	1.00	78.3
AS6074	Solid Foam Rigid Counterpart to WBSR	63.3	0.12	544.8	1	1.00	544.8
Unbraced F1D	Rubber Band Indoor Flyer	0.33	0.11	3.1	0.5	0.35	8.7
Silentius	Rubber Band Indoor Flyer	0.21	0.07	3.2	0.5	0.35	9.1
Fantasia	Rubber Band Indoor Flyer	0.21	0.06	3.2	0.5	0.35	9.2
A Day Fly	Full Scale HPH, Total Blade Area	34300	23.00	1491.3	10	31.62	47.2
Papillion A	Full Scale HPH, Total Blade Area	41200	25.00	1648.0	10	31.62	52.1
Papillion B	Full Scale HPH, Total Blade Area	42100	25.00	1684.0	10	31.62	53.3
Papillion C	Full Scale HPH, Total Blade Area	31400	19.30	1626.9	10	31.62	51.4
Yuri I	Full Scale HPH, Total Blade Area	37300	35.20	1059.7	10	31.62	33.5
Da Vinci III	Full Scale HPH, Blade Area of one Rotor	17000	6.84	2485.4	10	31.62	78.6

The resulting comparisons yielded mixed results. When compared with its solid foam counterpart (AS6074), the wire-braced rotor is much lighter weight, nearly seven times lighter. But compared with the ultralight rubber band aircraft, the wire-braced rotors were nearly seven times heavier. The favorable size-to-weight ratio compared

with foam structures was expected, but the great disparity with the indoor rubber band fliers was a surprise.

When compared with actual HPH rotor systems, the semi-rigid rotor model was essentially on par, slightly heavier than some for Japanese aircraft and virtually identical with Cal Poly's *Da Vinci III*, which seemed reasonable considering the coning of the unbraced model (tested and discussed in the next section) nearly mirrored the coning behavior of the *Da Vinci III* in its actual 1989 flight (depicted previously in Figures 1-4 and 2-4)

6.3   Individual Rotor Tests and Single Plane Rotor System Tests

The first series of hypotheses all deal with the ability of the ultra-light wire-braced rotors to maintain their geometry during rotational flight conditions.

6.3.1   Coning Results, Unbraced & Braced Rotors

The single rotor and single plane models were tested to measure their ability to resist the tendency to bend upward at the tips in a coning manner.

First, unbraced rotors were tested in a rotational condition. This was done both manually and on the static whirl stand at approximately 30 rpm (wing tip velocity 3 m/s). The performance was as expected with significant coning. (See Figure 6-2)
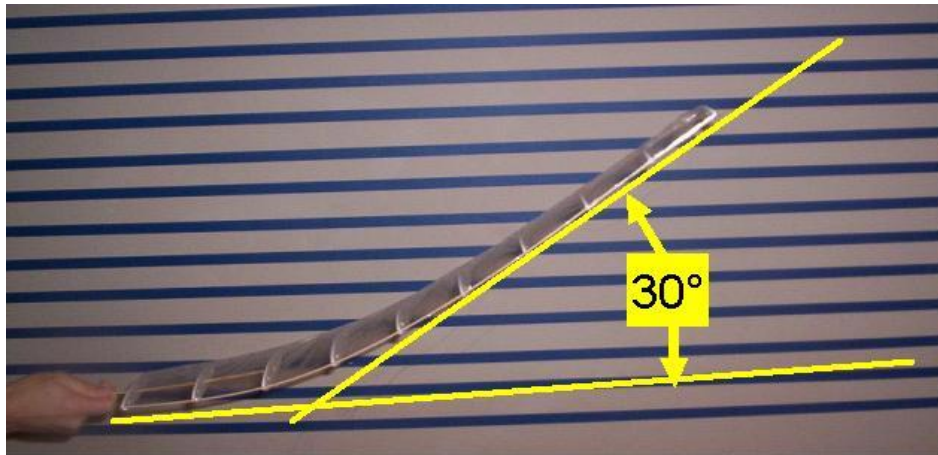
Figure 6-2 Unbraced Rotor in Rotation, 30° of Coning

Next, early tests of the wire-braced airfoils showed significant improvement over the unbraced rotors, as shown in Figure 6-3, yet some unfavorable coning (approximately 17°) was still measured.
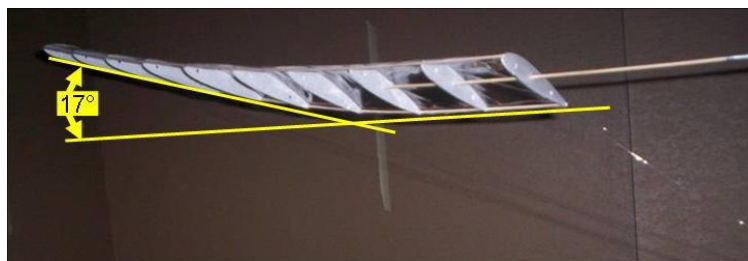
Figure 6-3 Initial Wire-braced Test, Still Minor Coning: 17° Local Coning

To compensate for the coning that was still observed, even with the wire braces, the rigging was adjusted, this time with a 10° anhedral angle, as shown in Figure 6-4.

Figure 6-4 Re-rigging Rotors to add 10° of Anhedral Angle

Subsequent manual tests and minor rigging adjustments resulted in tests producing no coning; the rotor plane was perpendicular to the axis of rotation and parallel to the ground. (See Figure 6-5)

Figure 6-5 Re-rigged Rotor Configuration, in Rotation, No Coning

6.3.2 Pitch Angle Control Results, Unbraced & Braced Rotors

As expected, without wire bracing to control the angle of attack along the span of the otherwise flexible airfoil, unruly pitch excursions proved were seen detrimental to efficient lift generation.

The first type of pitch excursion demonstrated was an increase in angle of attack, as shown in Figure 6-6, progressively increasing outboard from the center of the rotor.
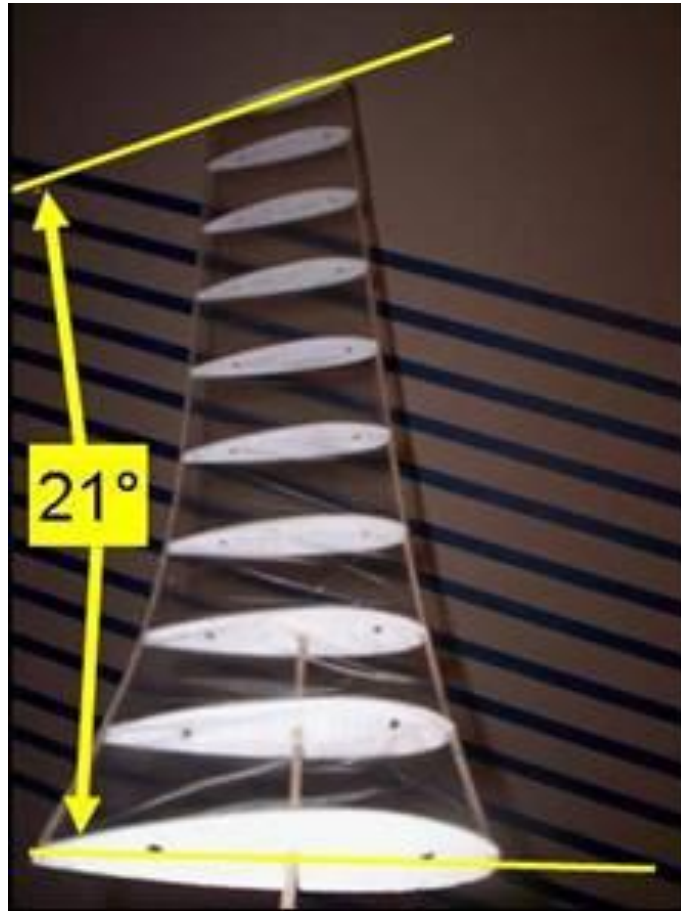
Figure 6-6 Positive Angle Pitch Excursion

The second type of pitch excursion observed was a gradually decreasing angle of attack, progressively decreasing moving outboard from the center of the rotor, as shown in Figure 6-7.
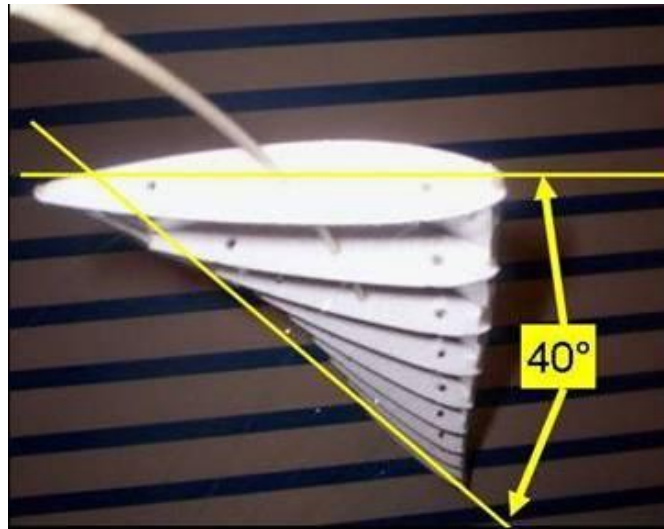
Figure 6-7 Negative Angle Pitch Excursion

With the rotors rigged with nylon bracing wires, desired angles of attack established during rigging were tested to see if they would maintain pitch geometry along the entire span of the airfoil during rotation. As shown in Figure 6-8, test showed that prescribed pitch angles all along the airfoil were maintained during rotational flight conditions.
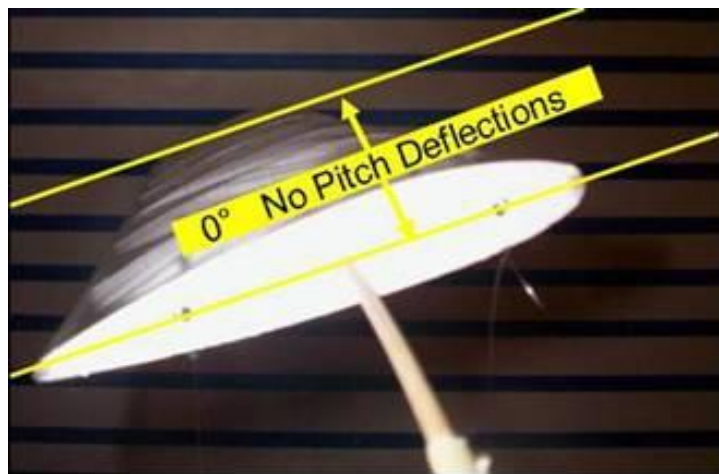
Figure 6-8 Wire-Braced Rotor, No Pitch Deviations

6.4 Coaxial Tests

In order to test the next pair of hypotheses,, coaxial interference and lifting forces, the coaxial model was loaded into the dynamic test stand.

6.4.1 Offset Interference, Avoiding Physical Collisions

No physical interference of the two rotor systems occurred during any of the coaxial testing. The offset distance between the two rotor planes proved sufficient to allow the two rotor systems to rotate independently of each other. At low speeds and minimal lift, the upper rotor system did not droop low enough to interfere with the lower rotor system. At higher rotational velocities the wire braces successfully restricted the rotors to their own plane—the lower rotor system did not cone up into the upper system. (See Figure 6-9)

Figure 6-9 Coaxial Rotors in Motion, No Interference

6.4.2 Lifting Force Results

The full coaxial model weighed approximately 1.35N (approximately 135g of force). In the stand, the full weight of the model was be borne by the force scale beneath.

Then, during flight tests, the lightening aircraft would lift off the scale and its overall weight would decrease, potentially all the way to 0 in a flight condition.

During the initial full power flight tests in the test stand, measured weights decreased from the fully loaded 135g to an observed low of only 3.7g (note: a measurement of 0g would indicate a free flight "liftoff" condition). While these were promising results, measurements did fluctuate and not enough data points were taken to be conclusive. (See Figure 6-10)

Observed Weight During Guided Flight Test #1

Weight on Scale (g) vs horizontal axis (0 to 6)
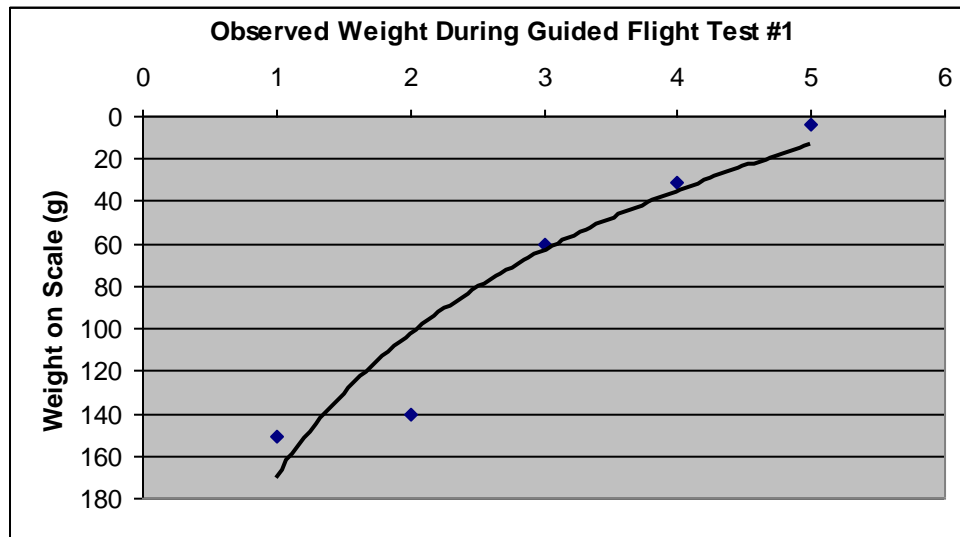
Figure 6-10 First Lifting Force Test

The next tests took more data points, revealed even greater fluctuations, and lower overall performance than the early tests, as shown in Figures 6-11 and 6-12.

Observed Weight During Guided Flight Test #2
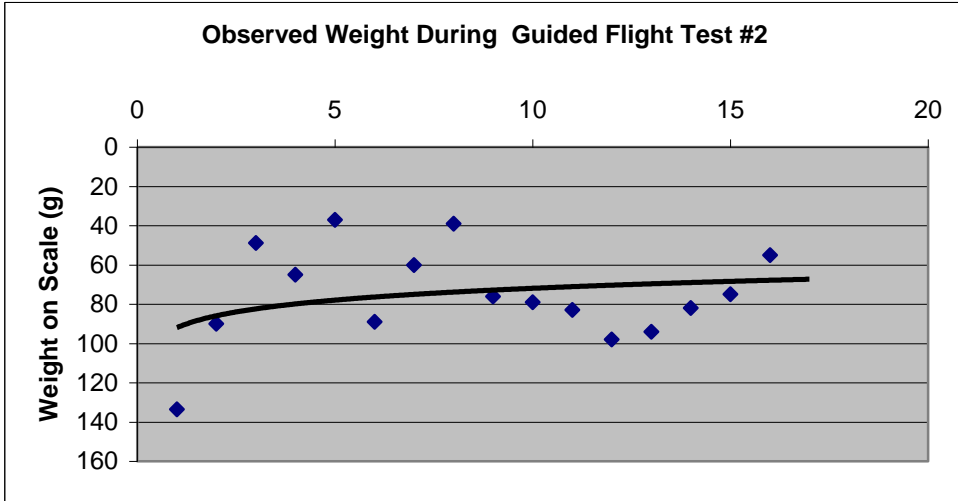
Figure 6-11 Lifting Force Test #2

Observed Weight During Guided Flight Test #3
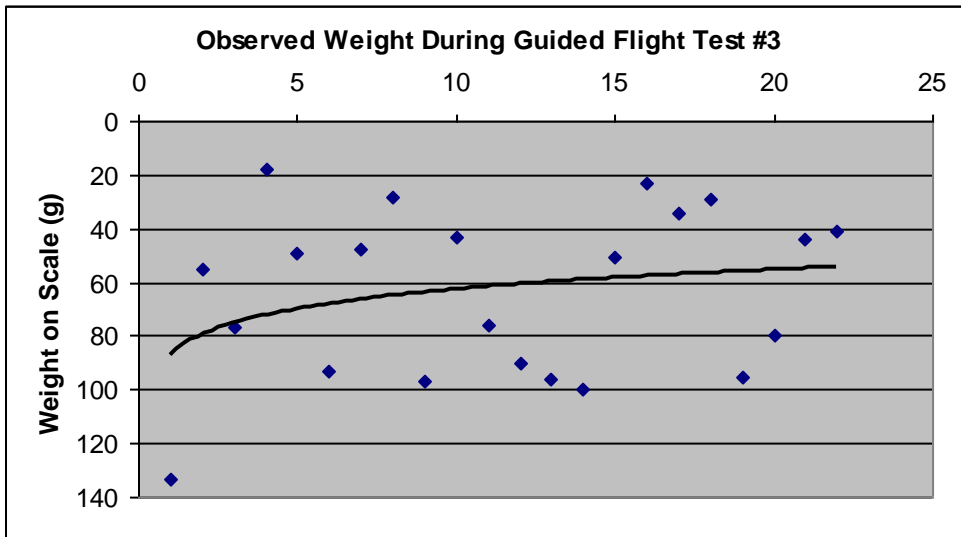
Figure 6-12 Lifting Force Test #3

A review of the sporadic performances in these two tests led to an assessment of possible causes. It was suspected that friction in the test stand, between the test stand's guide sleeve and the model's gearhead housing, as shown in Figure 6-13, was producing

a binding effect—both hampering observed lift and yielding the fluctuations in performance.
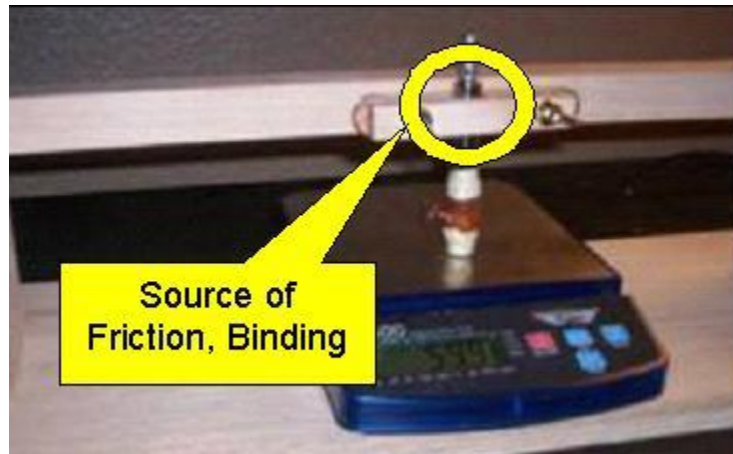
Figure 6-13 Test Stand Guide Sleeve

This friction and binding, not predicted during earlier functional checks, were apparently accentuated with the full model installed and in motion and with its long masts and wide rotors bending slightly off true perpendicular.

To help decrease the friction, a light coating of oil was applied to the test stand sleeve and to the gearhead.

An additional test was conducted with the now lubricated sleeve. This test resulted in far fewer fluctuations of performance, as shown in Figure 6-14, but there was still not sufficient lift to obtain hovering flight.
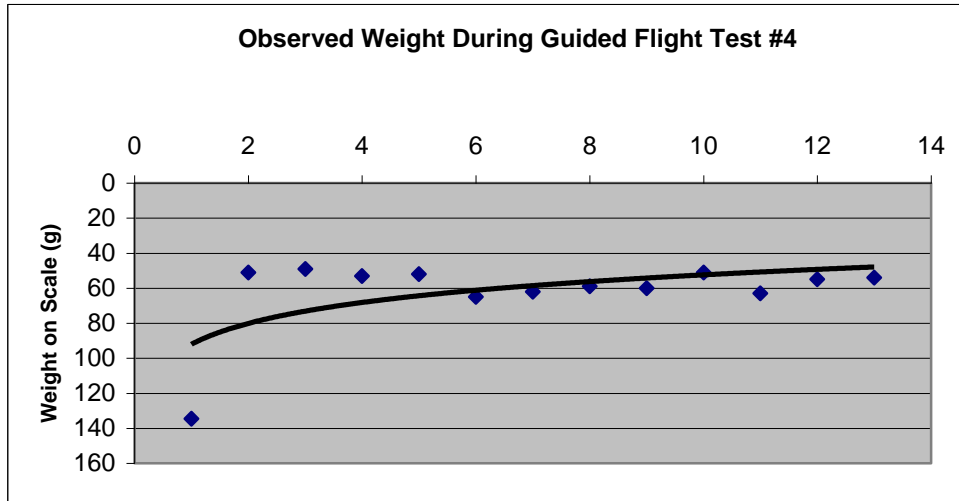
Figure 6-14 Lifting Force Test #4

6.5 Inherent Stability Tests

The purpose of these tests would have been to see if the fully operational coaxial flying model would have been self-stabilizing in terms of pitch and roll planes, and if it would not have drifted out of a given square meter footprint.

Unfortunately, the coaxial model never performed well enough to achieve a hovering flight. Therefore, the hypothesis for inherent stability was left untested.

6.6 Aerodynamic Drag from Bracing Wires

The analytical model used to predict the aerodynamic drag on each wire, utilized a segmental approach, dividing each bracing wire into .01m long theoretical segments. Based on the prescribed rotational velocity of approximately 30rpm, the relative speed for each segment was first calculated, based on its respective radius.

The segment's speed was then used to predict the coefficient of drag (Cd) based on the formulaic relationship of velocity and Cd presented in Figure 3-5.

58

The segment's Cd and size were then used to calculate the aerodynamic drag on the segment in Newtons (N).

The segment's drag was then included as a component of torque, in Newton meters (Nm).

Based on the segment's torque and its velocity, the power required or "power penalty" was then calculated for the wire segment in Watts (W)

These steps were then repeated for every .01m segment of all the model's 32 wires, factoring there respectvive lengths and angles. See Table 6-2 below for summary data and see Appendix A for additional details.

Table 6-2 Power Penalty due to Wire Drag, per Wire and Total

At 30 rpm	Power Required per Wire (W)	Power Reqd. for all 8 of Same Length/Angle
Wire #1	0.000	0.000
Wire #2	0.000	0.003
Wire #3	0.001	0.012
Wire #4	0.004	0.032
Total for all 32 wires (W)		0.048

As displayed in Table 6-2, the estimated power penalty from the drag of all 32 bracing wires on the coaxial model was approximately 0.05W. Which for this 1W system is a 5 percent penalty.

This drag penalty needed to be compared to whatever benefit was achieved due to structural weight savings allowed by the bracing wires. This is a subjective quantity, based on an optimized design, which the models measured and test in this thesis were not. However, an approximate break-even point could be calculated, based on the known

power penalty. For this scale model with a 100g design weight, the savings needed to overcome the wire drag power penalty would need to be at least 5g.

7 Conclusions and Recommendations

The following chapter first reviews the overall objectives of this thesis then considers the validity of each proposed hypothesis based on the performance testing results and analysis presented in the previous chapter. General conclusions are then drawn from the results. Lastly, recommendations for future research are established.

7.1.1 Review of Objectives

This thesis presents an original concept for a large, ultra lightweight rotor system that could be used on a potentially successful HPH. As conceived, the proposed rotor system would overcome the formidable and, thus far, insurmountable challenges to human-powered vertical flight by attempting to achieve the combination of an adeaquetly large rotor size, a sufficiently lightweight sturcture, and an inherently stable aircraft. The key features of the presented rotor system are concept are presented again in Figure 7-1, and are listed as follows:

- An elevated rotor system would enable external tensile bracing wires which would significantly decrease the internal structural requirements of the rotors and thus to reduce rotor weight

- The bracing wires would control airfoil geometry to prevent detrimental coning and unwanted twisting

- The wire-braced rotor system could to produce sufficient lift to enable hovering flight

- The elevated rotor system would provide a higher center of lift relative to the overall center of gravity (especially well above the heavy pilot-engine) and therefore provide a pendular self-stabilizing platform

- Analysis to demonstrate that the aerodynamic drag penalty induced by the external bracing wires would be more than offset by the decreased weight of the system.
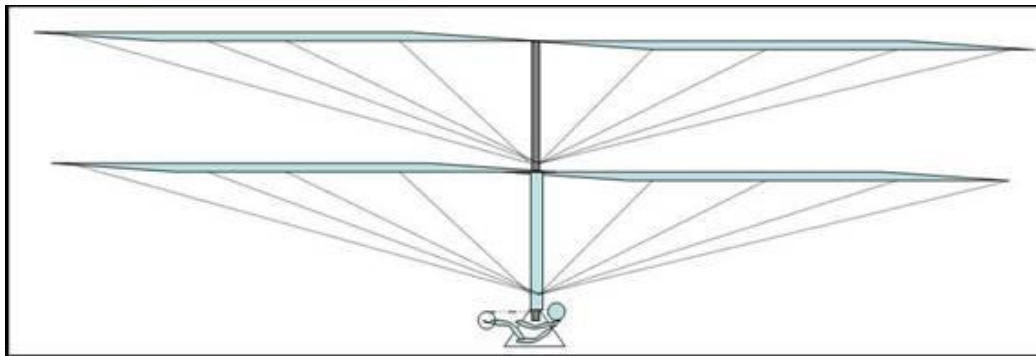
Figure 7-1 Proposed Concept for a Wire-braced Semi-rigid Coaxial Counter-rotating HPH

7.2   Testing the Hypotheses

Each key design feature of the proposed concept was the basis for one or more of the seven supporting hypotheses, as presented in Chapter 1. Each hypothesis was tested using either experimentation with physical scale models or with mathematical analysis.

In the following sections, each of the hypotheses is checked for validity based on the data, results, and analysis described in the previous chapter.

7.2.1 Hypothesis 1

Hypothesis 1 proposed that an elevated wire-braced rotor system could be "sufficiently lightweight" to support the design of a potentially successful HPH, as much as "five times lighter than a comparable rigid airfoil." Based on the mixed results presented in Table 6-1, this hypothesis appears inconclusive.

While the weight-to-surface area of the semi-rigid rotor model was nearly seven times lighter than a comparable rigid airfoil of the same size/geometry, the foam AS6074, it was also nearly 7 times heavier compared with the ultralight indoor rubber band flying models, and roughly equal to the full-sized HPH rotors.

7.2.2 Hypothesis 2

Hypothesis 2 proposed that the external wire bracing would "prevent rotor coning" and "keep the rotor system completely parallel to the ground." Based on the results of repeated whirl tests and flight attempts, this hypothesis appears valid. The wires prevented the rotors from coning and kept their attitude parallel to the ground. The wires could, in fact, be rigged to a range of possible lengths which could result in a correlating range of possible rotor flapping angles, from a dihedral to an anhedral angle. A parallel angle was the target orientation of this thesis.

7.2.3 Hypothesis 3

Hypothesis 3 proposed that the bracing wires would also control the "twisting and pitching angles of the rotor" and would "enable desired angles of attack all along the rotor." Test results showed that the pitch angle of the rotors could be successfully controlled all along the rotor span. The target test was to achieve a uniform angle of

attack, and this was repeatedly achieved after initial adjustments to rigging; the hypothesis appears valid. More complex geometries were not tested; however, it is reasonable to conclude that since the pitch angles could be controlled to achieve a parallel geometry, the angles could also be controlled to achieve more complex predetermined geometries as they varied along the rotor span.

7.2.4   Hypothesis 4

Hypothesis 4 proposed that the distance offset between the two rotor planes would "prevent physical interference of the two rotor discs." There were never any physical collisions or even near misses between the two rotor planes during coaxial testing. This hypothesis appears valid

7.2.5   Hypothesis 5

Hypothesis 5 proposed that the rotors would "generate sufficient lift so as to achieve hovering flight." This hypothesis is inconclusive. While the coaxial model never did fully takeoff to a hover, lifting force tests did show substantial lift was generated.

7.2.6   Hypothesis 6

Hypothesis 6 proposed that an "elevated rotor system would be inherently stable, placing the relatively heavy pilot-engine far below the center of lift to create a pendulum type of stability. This hypothesis could not be tested since the coaxial model never achieved enough lift for free flight.

7.2.7   Hypothesis 7

Hypothesis 7 proposed that the aerodynamic drag penalty induced by the bracing wires would be "more than offset by the power saved through reduced airfoil weight afforded by the bracing wires."   The total power penalty for the coaxial model was calculated to be approximately 0.05W, which compared to a total system power of just 1W, is only a 5 percent penalty.

The ultralight wire-braced wings were each 7 times lighter weight than their rigid rotor counterpart, which for this model would equate to a remarkable weight savings (over 200 grams).   However since other wings were later reviewed with an even lower weight-to-surface area ratio than the wire-braced rotors (see Table 6-1), additional testing and an optimized design would need to be performed to validate that the wire bracing would still be advantageous.   Therefore, this hypothesis remains inconclusive.

7.3   General Conclusions

The wire bracing was clearly successful in controlling the geometry of a flexible rotor in terms of coning and pitch.   The semi-rigid rotors were indeed lighter in weight than its rigid counterpart; however since further review found even lighter weight wings used in rubber band model aircraft. (Gitlow 1993)

The key conclusion is that wire-bracing is a reasonable, feasible, and potentially advantageous system for a helicopter that would require very large, lightweight rotors, otherwise flexible rotors, such as an HPH.

7.4 Recommendations:

There are several areas of research that could significantly refine the concepts of the wire-braced semi-rigid elevated rotor system. The following is a list of recommended areas of research and development:

7.4.1 Optimal Airfoil Design

A key recommendation for future research would be to perform a thorough aerodynamic analysis to design optimally efficient rotors that could incorporate the design concepts of a wire-braced semi-rigid elevated rotor system as presented in this thesis. This could enable the manufacture of airfoils that would otherwise be prohibitively large, weak, and flexible, yet aerodynamically optimum. Design analysis should be performed for additional scale model testing and then for an operational full-size HPH configuration.

7.4.2 Drive System

An efficient drive system will need to be developed in order to drive a coaxial system.

7.4.3 Material Selection

A review of appropriate materials should be performed in order to further optimize the system, both at the scale model level and for a potential full-sized vehicle. The trade study should consider optimal mechanical performance (strength, weight) and also consider cost, availability, ease of manufacture, and reparability.

7.4.4 Active Rigging

All wire bracing used in this study was of fixed length with the intent of holding the rotors in a predetermined orientation. However, the wire lengths could be actively adjusted during flight, either to refine performance or to make deliberate pitch changes to either increase or decrease lift.

7.4.5 Practical Applications

While the impetus for this study was to further pursue the Sikorsky Prize for a human-powered helicopter, research should be performed on potential practical/commercial applications of large wire-braced rotors, such as:

- Heavy-lift industrial applications

- High altitude/thin atmosphere flight operations

8   References

American Institute of Aeronautics and Astronautics, Leonardo Da Vinci, (2008).
Available from http://www.aiaa.org/content.cfm?pageid=425; Internet, accessed
November 13, 2008.

Burke, J. D. (1980). *The Gossamer Condor and Albatross: A Case Study in Aricraft
Design*. AIAA Professional Series, AeroVironment Inc.

Cal Poly, The History of the Human Powered Helicopter Project. (2008). Available from
http://www.calpoly.edu/~wpatters/helo.html; Internet, accessed November 13,
2008.

Cranfield, A. D. (1987). "Pedaling towards a vertical take-off," *CME*, September 1987,
58-60.

Drees, J. M. (1993).   "The Human-powered helicopter challenge," *Vertiflite*,
January/February 1993, 32-34.

Drees, J. M. (1995).   "Human-powered helicopter challenge heats up!" *Vertiflite*,
January/February 1995, 32-34.

Drela, M. (1988). "Low-Reynolds-number airfoil design for the M.I.T. Daedalus
prototype: a case study," *Journal of Aircraft*, 25, 724-732.

Dryden Flight Research Center, Images and Description of the MIT Daedalus Project,
(2008), available from
http://www.dfrc.nasa.gov/Gallery/Photo/Daedalus/index.html; Internet; accessed
13 November 2008.

Faulhaber Online Catalog. (2008). Available from http://www.micromo.com; Internet;
accessed November 13, 2008.

Filippone, A. (2002). "The human-powered helicopter." *The Aeronautical Journal*,
November 2002, 613-618.

Furton, D. (2004). "Experimental Aircraft, Helios: a helicopter with legs," *Aviation
Today,* Retrieved November 23, 2004.

Gavaghan, H. (1989) "Pedal power lifts helicopter into history . . ." *New Scientist,* 23, 24.

Grosser, M. (1991) *Gossamer Odysssey: The Triumph of Human-Powered Flight*. Dover Publications.

Grossmann, J. (1988). "Hover story, one minute and three meters to glory," *Air & Space*, June/July 1988, 84-93.

Human Powered Helicopters, Images and Specifications of Aircraft, November 13, 2008, available from http://www.humanpoweredhelicopters.org; Internet; accessed 13 November 2008.

Hansworth, J. (2004). "Human-powered helicopter grounded," *CNEWS*. Retrieved November 23, 2004, cnews.canoe.ca.

Larwood, S. (1990) "Aerodynamic design of the Cal Poly Da Vinci human-powered helicopter." Retrieved November 13, 2008, http://www.humanpoweredhelicopters.org/articles/LarwoodSaiki1990.pdf

Mouritsen, S. (1990). An Aerodynamic and Design Analysis of the Human Powered Helicopter. SAWE Paper 4 Society of Allied Weight Engineers, Inc.

Munson, B. R., Young, D. F., Okiishi, T. H. (1993). *Fundamentals of Fluid Mechanics Second Edition.* John Wiley and Sons Inc.

Naito, A. (1990). *A Study of Human Powered Helicopter in Japan.* SAWE Paper 1925, Society of Allied Weight Engineers, Inc.

Raskin, J. (2007). "A good Airfoil for Small RC Models. Retrieved January 2, 2007, jef.raskincenter.org/published/airfoil.html.

Seddon, J., Newman, S. (2001). *Basic Helicopter Aerodynamics Second Addition*, American Institute of Aeronautics and Astronautics, Inc.

Sopher, R. (1997). "The AHS Igor Sikorsky Human Powered Helicopter Competition," *Vertiflite*, May/June 1997, 32-34.

Taylor, R. (1995). *The First Human-Powered Flight*. Franklin Watts.

Trayling, G. (1989). "A human-powered helicopter: design considerations," The Technical Journal of the IHPVA, 24, 9-11.

APPENDIX

Appendix A. Wire Drag Penalty Analysis

Radial Length (m)	Delta r (m)	Speed (m/s)	Cd(v)	Drag (N)	Torque (N-m)	Power Required to move (Watts)	Power Reqd ~ for longer Hypotenuse Length			
							Wire #1	Wire #2	Wire #3	Wire #4
0.01	0.01	0.031415927	17.55709	0.0000000	0.0000000	0.0000000	0.0000000	0.0000000	0.0000000	0.0000000
0.02	0.01	0.062831853	13.06089	0.0000001	0.0000000	0.0000000	0.0000000	0.0000000	0.0000000	0.0000000
0.03	0.01	0.09424778	10.98543	0.0000001	0.0000000	0.0000000	0.0000000	0.0000000	0.0000000	0.0000000
0.04	0.01	0.125663706	9.716129	0.0000002	0.0000000	0.0000000	0.0000000	0.0000000	0.0000000	0.0000000
0.05	0.01	0.157079633	8.833485	0.0000003	0.0000000	0.0000000	0.0000001	0.0000000	0.0000000	0.0000000
0.06	0.01	0.184495559	8.172173	0.0000004	0.0000000	0.0000001	0.0000001	0.0000001	0.0000001	0.0000001
0.07	0.01	0.219911486	7.651818	0.0000005	0.0000000	0.0000001	0.0000001	0.0000001	0.0000001	0.0000001
0.08	0.01	0.251327412	7.227926	0.0000006	0.0000000	0.0000001	0.0000002	0.0000001	0.0000001	0.0000001
0.09	0.01	0.282743339	6.873561	0.0000007	0.0000001	0.0000002	0.0000002	0.0000002	0.0000002	0.0000002
0.1	0.01	0.314159265	6.571318	0.0000008	0.0000001	0.0000003	0.0000003	0.0000003	0.0000003	0.0000003
0.11	0.01	0.345575192	6.309371	0.0000009	0.0000001	0.0000003	0.0000004	0.0000003	0.0000003	0.0000003
0.12	0.01	0.376991118	6.079361	0.0000011	0.0000001	0.0000004	0.0000005	0.0000004	0.0000004	0.0000004
0.13	0.01	0.408407045	5.875184	0.0000012	0.0000002	0.0000005	0.0000006	0.0000005	0.0000005	0.0000005
0.14	0.01	0.439822972	5.692264	0.0000014	0.0000002	0.0000006	0.0000007	0.0000006	0.0000006	0.0000006
0.15	0.01	0.471238898	5.527093	0.0000015	0.0000002	0.0000007	0.0000009	0.0000008	0.0000007	0.0000007
0.16	0.01	0.502654825	5.376926	0.0000017	0.0000003	0.0000008	0.0000010	0.0000009	0.0000009	0.0000009
0.17	0.01	0.534070751	5.239585	0.0000018	0.0000003	0.0000010	0.0000012	0.0000010	0.0000010	0.0000010
0.18	0.01	0.565486678	5.113311	0.0000020	0.0000004	0.0000011	0.0000014	0.0000012	0.0000012	0.0000011
0.19	0.01	0.596902604	4.996668	0.0000022	0.0000004	0.0000013	0.0000016	0.0000014	0.0000013	0.0000013
0.2	0.01	0.628318531	4.888469	0.0000024	0.0000005	0.0000015	0.0000018	0.0000016	0.0000015	0.0000015
0.21	0.01	0.659734457	4.787726	0.0000026	0.0000005	0.0000017	0.0000020	0.0000018	0.0000017	0.0000017
0.22	0.01	0.691150384	4.693604	0.0000028	0.0000006	0.0000019	0.0000023	0.0000020	0.0000020	0.0000019
0.23	0.01	0.72256631	4.605397	0.0000030	0.0000007	0.0000021	0.0000026	0.0000023	0.0000022	0.0000022
0.24	0.01	0.753982237	4.522497	0.0000032	0.0000008	0.0000024	0.0000029	0.0000025	0.0000025	0.0000024
0.25	0.01	0.785398163	4.444385	0.0000034	0.0000008	0.0000026	0.0000032	0.0000028	0.0000027	0.0000027
0.26	0.01	0.81681409	4.370608	0.0000036	0.0000009	0.0000029	0.0000035	0.0000031	0.0000030	0.0000030
0.27	0.01	0.848230016	4.300772	0.0000038	0.0000010	0.0000032	0.0000039	0.0000034	0.0000033	0.0000033
0.28	0.01	0.879645943	4.234532	0.0000040	0.0000011	0.0000035	0.0000043	0.0000038	0.0000036	0.0000036
0.29	0.01	0.911106187	4.171584	0.0000043	0.0000012	0.0000039	0.0000047	0.0000041	0.0000040	0.0000039
0.3	0.01	0.942477796	4.111659	0.0000045	0.0000013	0.0000042	0.0000051	0.0000045	0.0000044	0.0000043
0.31	0.01	0.973893723	4.054519	0.0000047	0.0000015	0.0000046		0.0000049	0.0000047	0.0000047
0.32	0.01	1.005309649	3.999949	0.0000050	0.0000016	0.0000050		0.0000053	0.0000051	0.0000050
0.33	0.01	1.036725576	3.94776	0.0000052	0.0000017	0.0000054		0.0000057	0.0000056	0.0000055
0.34	0.01	1.068141502	3.89778	0.0000055	0.0000019	0.0000058		0.0000062	0.0000060	0.0000059
0.35	0.01	1.099557429	3.849854	0.0000057	0.0000020	0.0000063		0.0000067	0.0000065	0.0000064
0.36	0.01	1.130973355	3.803843	0.0000060	0.0000022	0.0000068		0.0000072	0.0000070	0.0000069
0.37	0.01	1.162389282	3.75962	0.0000062	0.0000023	0.0000073		0.0000077	0.0000075	0.0000074
0.38	0.01	1.193805208	3.717071	0.0000065	0.0000025	0.0000078		0.0000083	0.0000080	0.0000079
0.39	0.01	1.225221135	3.67609	0.0000068	0.0000026	0.0000083		0.0000088	0.0000085	0.0000084
0.4	0.01	1.256637061	3.636581	0.0000071	0.0000028	0.0000089		0.0000094	0.0000091	0.0000090
0.41	0.01	1.288052988	3.598457	0.0000073	0.0000030	0.0000095		0.0000100	0.0000097	0.0000096
0.42	0.01	1.319468915	3.561637	0.0000076	0.0000032	0.0000101		0.0000107	0.0000103	0.0000102
0.43	0.01	1.350884841	3.526047	0.0000079	0.0000034	0.0000107		0.0000113	0.0000110	0.0000109
0.44	0.01	1.382300768	3.491619	0.0000082	0.0000036	0.0000113		0.0000120	0.0000117	0.0000115
0.45	0.01	1.413716694	3.45829	0.0000085	0.0000038	0.0000120		0.0000127	0.0000124	0.0000122
0.46	0.01	1.445132621	3.426001	0.0000088	0.0000040	0.0000127		0.0000135	0.0000131	0.0000129
0.47	0.01	1.476548547	3.394698	0.0000091	0.0000043	0.0000134		0.0000143	0.0000138	0.0000137
0.48	0.01	1.507964474	3.364331	0.0000094	0.0000045	0.0000142		0.0000151	0.0000146	0.0000144
0.49	0.01	1.5393804	3.334854	0.0000097	0.0000048	0.0000150		0.0000159	0.0000154	0.0000152
0.5	0.01	1.570796327	3.306223	0.0000100	0.0000050	0.0000158		0.0000167	0.0000162	0.0000160
0.51	0.01	1.602212253	3.278397	0.0000104	0.0000053	0.0000166		0.0000176	0.0000170	0.0000168
0.52	0.01	1.63362818	3.251339	0.0000107	0.0000055	0.0000174		0.0000185	0.0000179	0.0000177
0.53	0.01	1.665044106	3.225014	0.0000110	0.0000058	0.0000183		0.0000194	0.0000188	0.0000186
0.54	0.01	1.696460033	3.199387	0.0000113	0.0000061	0.0000192		0.0000204	0.0000198	0.0000195
0.55	0.01	1.727875959	3.17443	0.0000117	0.0000064	0.0000201		0.0000214	0.0000207	0.0000205
0.56	0.01	1.759291886	3.150111	0.0000120	0.0000067	0.0000211		0.0000224	0.0000217	0.0000214
0.57	0.01	1.790707813	3.126404	0.0000123	0.0000070	0.0000221		0.0000234	0.0000227	0.0000224
0.58	0.01	1.822123739	3.103283	0.0000127	0.0000074	0.0000231			0.0000237	0.0000235
0.59	0.01	1.853539666	3.080724	0.0000130	0.0000077	0.0000241			0.0000248	0.0000245
0.6	0.01	1.884955592	3.058705	0.0000134	0.0000080	0.0000252			0.0000259	0.0000256
0.61	0.01	1.916371519	3.037202	0.0000137	0.0000084	0.0000263			0.0000270	0.0000267
0.62	0.01	1.947787445	3.016197	0.0000141	0.0000087	0.0000274			0.0000282	0.0000278
0.63	0.01	1.979203372	2.99567	0.0000144	0.0000091	0.0000286			0.0000294	0.0000290
0.64	0.01	2.010619298	2.975602	0.0000148	0.0000095	0.0000297			0.0000306	0.0000302
0.65	0.01	2.042035225	2.955977	0.0000152	0.0000099	0.0000310			0.0000318	0.0000314
0.66	0.01	2.073451151	2.936778	0.0000155	0.0000102	0.0000322			0.0000331	0.0000327
0.67	0.01	2.104867078	2.91799	0.0000159	0.0000107	0.0000335			0.0000344	0.0000340
0.68	0.01	2.136283004	2.899597	0.0000163	0.0000111	0.0000348			0.0000357	0.0000353
0.69	0.01	2.167698931	2.881587	0.0000167	0.0000115	0.0000361			0.0000371	0.0000367
0.7	0.01	2.199114858	2.863945	0.0000170	0.0000119	0.0000375			0.0000385	0.0000381
0.71	0.01	2.230530784	2.846659	0.0000174	0.0000124	0.0000389			0.0000399	0.0000395
0.72	0.01	2.261946711	2.829717	0.0000178	0.0000128	0.0000403			0.0000414	0.0000409
0.73	0.01	2.293362637	2.813107	0.0000182	0.0000133	0.0000417			0.0000429	0.0000424
0.74	0.01	2.324778564	2.796819	0.0000186	0.0000138	0.0000432			0.0000444	0.0000439
0.75	0.01	2.35619449	2.780842	0.0000190	0.0000142	0.0000447			0.0000460	0.0000454
0.76	0.01	2.387610417	2.765166	0.0000194	0.0000147	0.0000463			0.0000476	0.0000470
0.77	0.01	2.419026343	2.749782	0.0000198	0.0000152	0.0000479			0.0000492	0.0000486
0.78	0.01	2.45044227	2.73468	0.0000202	0.0000158	0.0000495			0.0000509	0.0000503
0.79	0.01	2.481858196	2.719852	0.0000206	0.0000163	0.0000511			0.0000526	0.0000520
0.8	0.01	2.513274123	2.705289	0.0000210	0.0000168	0.0000528			0.0000543	0.0000537
0.81	0.01	2.544690049	2.690984	0.0000214	0.0000174	0.0000545			0.0000561	0.0000554
0.82	0.01	2.576105976	2.676928	0.0000219	0.0000179	0.0000563			0.0000579	0.0000572
0.83	0.01	2.607521902	2.663115	0.0000223	0.0000185	0.0000580			0.0000597	0.0000590
0.84	0.01	2.638937829	2.649538	0.0000227	0.0000191	0.0000599			0.0000616	0.0000608
0.85	0.01	2.670353756	2.636189	0.0000231	0.0000197	0.0000617				0.0000627
0.86	0.01	2.701769682	2.623062	0.0000236	0.0000203	0.0000636				0.0000646
0.87	0.01	2.733185609	2.610151	0.0000240	0.0000209	0.0000656				0.0000666
0.88	0.01	2.764601535	2.597451	0.0000244	0.0000215	0.0000675				0.0000686
0.89	0.01	2.796017462	2.584954	0.0000249	0.0000221	0.0000695				0.0000706
0.9	0.01	2.827433388	2.572656	0.0000253	0.0000228	0.0000715				0.0000727
0.91	0.01	2.858849315	2.560552	0.0000257	0.0000234	0.0000736				0.0000748
0.92	0.01	2.890265241	2.548636	0.0000262	0.0000241	0.0000757				0.0000769
0.93	0.01	2.921681168	2.536904	0.0000266	0.0000248	0.0000778				0.0000791
0.94	0.01	2.953097094	2.52535	0.0000271	0.0000255	0.0000800				0.0000813
0.95	0.01	2.984513021	2.51397	0.0000275	0.0000262	0.0000822				0.0000835
0.96	0.01	3.015928947	2.50276	0.0000280	0.0000269	0.0000844				0.0000858
0.97	0.01	3.047344874	2.491715	0.0000285	0.0000276	0.0000867				0.0000881
0.98	0.01	3.078760801	2.480831	0.0000290	0.0000283	0.0000890				0.0000905
0.99	0.01	3.110176727	2.470105	0.0000294	0.0000291	0.0000914				0.0000929
1	0.01	3.141592654	2.459532	0.0000299	0.0000299	0.0000938				0.0000953
1.01	0.01	3.17300858	2.449109	0.0000303	0.0000306	0.0000962				0.0000978
1.02	0.01	3.204424507	2.438832	0.0000308	0.0000314	0.0000987				0.0001003
1.03	0.01	3.235840433	2.428698	0.0000313	0.0000322	0.0001012				0.0001028
1.04	0.01	3.26725636	2.418704	0.0000318	0.0000330	0.0001038				0.0001054
1.05	0.01	3.298672286	2.408845	0.0000322	0.0000339	0.0001063				0.0001080
1.06	0.01	3.330088213	2.39912	0.0000327	0.0000347	0.0001090				0.0001107
1.07	0.01	3.361504139	2.389525	0.0000332	0.0000355	0.0001116				0.0001134
1.08	0.01	3.392920066	2.380056	0.0000337	0.0000364	0.0001143				0.0001162
1.09	0.01	3.424335992	2.370712	0.0000342	0.0000373	0.0001171				0.0001189
1.1	0.01	3.455751919	2.36149	0.0000347	0.0000382	0.0001199				0.0001218
1.11	0.01	3.487167845	2.352386	0.0000352	0.0000391	0.0001227				0.0001246
1.12	0.01	3.518583772	2.343399	0.0000357	0.0000400	0.0001256				0.0001275
						Subtotals	0.0000455	0.0003855	0.0014782	0.0040619
						Qty per Aircaft	8	8	8	8
						Subtotals	0.000364321	0.003083682	0.011825912	0.032495345
						Grand total W		0.05		